The repertoire of resistance mutations selected by a *Pseudomonas aeruginosa* type IV pilus-targeting lytic bacteriophage

Veronica N. Tran, Hanjeong Harvey, Tanisha S. Lahane, and Lori L. Burrows*

Department of Biochemistry and Biomedical Sciences and the Michael G. DeGroote Institute for Infection Disease Research, McMaster University

*For correspondence: lori.burrows@mcmaster.ca

ABSTRACT

P. aeruginosa type IV pili (T4P) are complex surface-exposed nanomachines used for twitching motility and biofilm formation. Exposure to bacteriophages that use T4P as their primary receptor can select for resistance mutations that reduce or abolish pilus expression. Since T4P are important virulence factors, such loss can affect pathogenicity and fitness, desirable outcomes for phage therapy. Here, we evaluated the repertoire of mutations in *P. aeruginosa* PAO1 exposed to the pilus-specific lytic phage PO4 and their ability to revert after removal of phage. Resistant isolates ranged from hyperpiliated to bald, but none retained twitching motility. We focused on isolates that still expressed surface pili, including one with an internal 4-amino acid duplication in the essential prepilin peptidase/methyltransferase, PilD. This duplication, distal to the predicted active sites, delayed prepilin processing. Accumulation of unprocessed subunits suppressed expression of new prepilins via inhibition of PilSR two-component system activity, restricting availability of functional subunits and conferring phage resistance. Introduction of a PilS point mutation that makes cells insensitive to accumulation of unprocessed pilins restored motility and phage susceptibility. Of the mutants tested, only those with a duplication in *pilD* recovered wild-type motility following removal of phage pressure, likely through slip-strand mispairing as a codon-modified variant did not revert. This work shows that resistance to pilus-specific phages does not require loss of pilus expression, and certain mutations can allow bacteria to regain pilus function. Characterizing spontaeous mutations selected by phages can help to define the function and vulnerabilities of the type IV pilus system.

SIGNIFICANCE

As use of phages to treat antibiotic-resistant pathogens such as *Pseudomonas aeruginosa* increases, it is important to understand potential outcomes of phage exposure. Most therapeutic *P. aeruginosa* phages use lipopolysaccharides (LPS) or T4P as primary receptors. Studying the properties of strains resistant to T4P-targeting phages can guide the design of phage cocktails to mitigate treatment resistance. We show that depending on the mutation, some phage-resistant strains can revert to wild-type sequences, emphasizing the importance of combining diverse phages to supress resurgence. By characterizing mutations that confer resistance, we can better understand whether pilus structural or regulatory components are more likely to be lost. Using phages to select for loss of pilus function represents an unbiased approach to identify new mutations in pilus-related proteins, shedding light on understudied components. Building a database of such mutations will help guide strategies to target and disarm this key *P. aeruginosa* virulence factor.

INTRODUCTION

Type IV pili (T4P) are the most common type of prokaryotic surface adhesin and are involved in motility, surface sensing, and DNA uptake (1–3). These hair-like filaments allow for non-specific attachment of bacterial pathogens to surfaces and contribute to establishment of infection and dissemination of pathogens in plant and animal hosts (4–6). They also serve as receptors for select bacteriophages (phages) that bind to the pili to initiate their infection cycle (7–9). Here we investigated the effects of exposing *Pseudomonas aeruginosa* to a T4P-targeting phage, focusing on mechanisms of resistance and potential for reversion to wild-type phenotypes following removal of the phage.

P. aeruginosa is an opportunistic antibiotic-resistant pathogen considered by the World Health Organization to be a top priority for development of new therapies, and a model species for the study of T4P biology (3, 10). There are 3 major subfamilies of T4P: T4aP, T4bP, and T4cP (Tad), and most *P. aeruginosa* strains express T4aP (2, 11). T4aP are repeatedly and rapidly extended and retracted by a complex nanomachine that spans the entire cell envelope (**Figure 1**). Major pilins (PilA) are lollipop-shaped subunits that make up the length of the pilus, while the minor pilin complex, consisting of minor pilins FimU, PilVWX and PilE, plus the non-pilus adhesin PilY1, is located at the tip (3, 12). Both major and minor pilins are initially expressed as inner membrane-embedded prepilins, with a short, positively charged leader sequence that is cleaved on the cytoplasmic side of the membrane by the prepilin peptidase PilD, followed by methylation of the new N-terminus, also by PilD (13, 14). Maturation of pilins by removal of the leader sequence is essential to make them competent for assembly, while methylation is not (15, 16).

After formation of a minor pilin tip complex in the cytoplasmic membrane, mature pilins are added sequentially from inner membrane pools to the base of the complex, and the pilus is thus extended through the periplasm and out of the cell (3). Retraction reverses this process, disassembling the filament and returning the major pilins to the membrane to be used for subsequent rounds of extension (3, 17). Extension and retraction are powered by the extension ATPase PilB and retraction ATPases PilT and PilU, respectively, and coordinated by the platform protein PilC (18–22). The inner-membrane alignment subcomplex (PilMNOP) and the outer membrane secretin channel (PilQ) form a gated conduit that guides the growing pilus through the cell envelope (23–26).

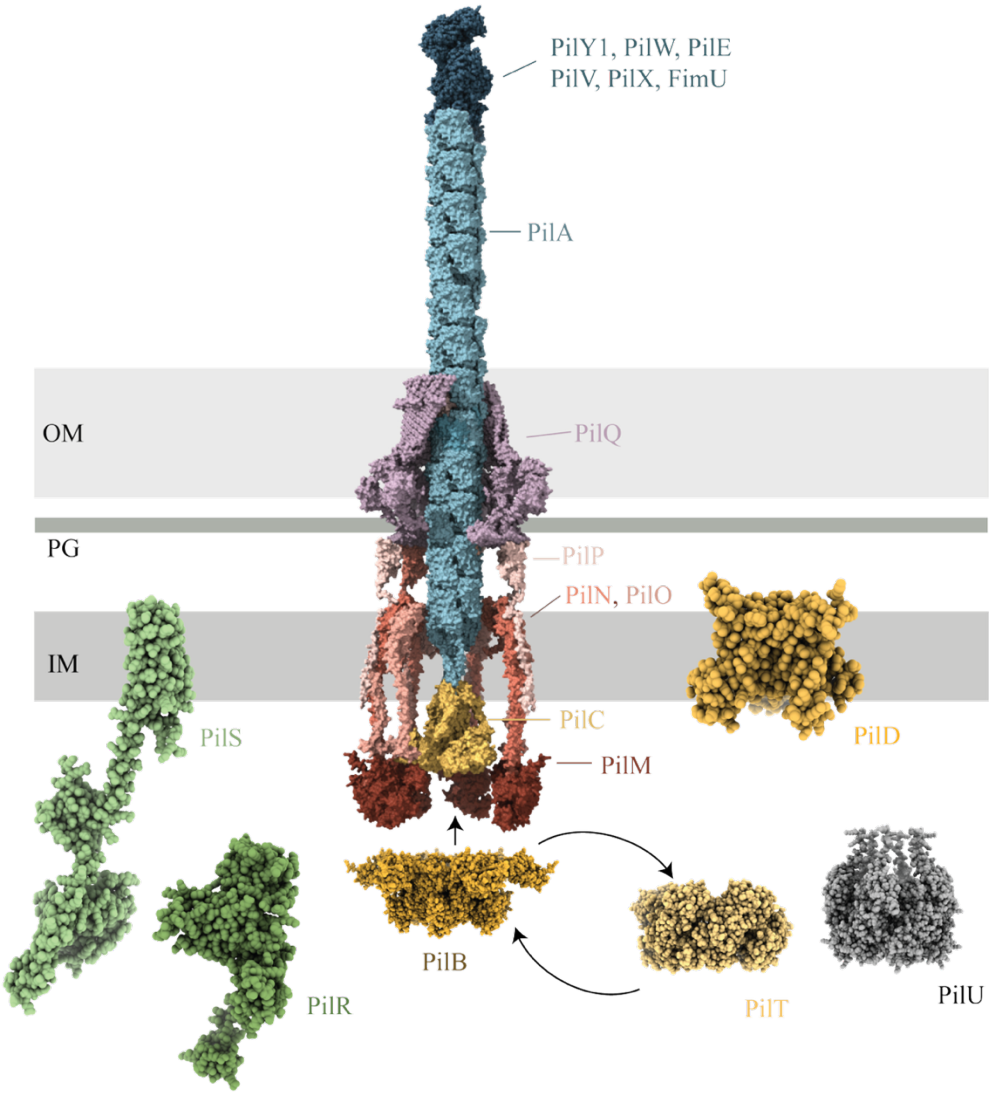

Figure 1. Structural models of the type IV pilus machinery. The type IV pilus is assembled by a complex protein nanomachine (EMD-43426) composed of four subcomplexes. The outer membrane secretin (PilQ) is shown in purple, the alignment subcomplex (PilM, PilN, PilO, PilP) in red, inner membrane motor subcomplex (PilC, PilB [AlphaFold3], PilT [PDB: 3JVU], PilU [grey, AlphaFold3], PilD [AlphaFold3]) in yellow and orange. PilB and PilT both interact with PilC, but not simultaneously, as indicated by the alternating arrows.The pilus subcomplex (major pilin subunits PilA and minor pilin subcomplex PilY1, PilE, PilW, PilV, PilX, FimU [AlphaFold3]) are shown in blue. The PilS-PilR two component system (green, AlphaFold3) regulates *pilA* expression. Coloured subcomplexes and labels indicate components in which we identified mutations conferring phage resistance. AlphaFold3 model confidence information is available in **Supplementary Figure 1.** Models are not to scale.

Pilus extension and retraction facilitates a form of movement on surfaces called twitching motility (27), and twitching-deficient cells have reduced virulence, impaired ability to infect, and form abnormal biofilm structures (3, 28). Phages that use the pilus as a primary receptor take advantage of its retraction to gain access to the cell surface, where they may interact with secondary receptors and inject their genetic material (18, 29, 30). Such phages may bind to the

major, or more rarely, the minor pilins (9, 31) although the specific molecular details of recognition and binding are only beginning to emerge (32).

Phages and bacteria are in an ongoing arms race, with each adapting as the other evolves new means of escape. Bacterial resistance mechanisms act at all stages of phage infection, including initial phage adsorption, which is thought to occur stochastically (33). Phage receptors can be mutated, post-translationally modified, masked by polysaccharides, or their surface chemistry or length altered to avoid phage infection (9, 34, 35). These changes can have implications for bacterial fitness, virulence, and recognition by the immune system, as well as the design of interventions. With antibiotic resistance on the rise, phage therapy is being revisited for treatment of persistent infections (36). Therefore, it is important to understand how bacteria might respond to and evade phage infection through surface modifications. In a clinical context, T4P-targeting phages could be used to steer infecting strains towards reduced fitness and/or increased susceptibility to treatment through loss of T4P function (37, 38). However, selection for mutations that could easily revert (e.g. phase variants or sequence duplications) or that could be bypassed by suppressors may allow for return to virulence once phage therapy is completed.

Here we examined the repertoire and potential reversibility of mutations conferring resistance following exposure of *P. aeruginosa* PAO1 to PO4, a T4P-targeting lytic phage (7). Phage-resistant mutants (PRMs) were sequenced to identify relevant mutations, and the ability of those mutations to confer cross-resistance to other phages tested. Unique resistance mutations in multiple regulatory and structural genes were identified, including a novel duplication in the essential prepilin peptidase PilD that led to protracted delays in cleavage of its prepilin substrates. Since most of the mutations identified were point mutations, small insertions/deletions (indels) or short sequence duplications, adaptation in the absence of phage pressure was evaluated. This analysis provided a snapshot of the range and stability of phage-selected T4aP mutations, important information for future design of phage cocktails.

RESULTS

T4aP-targeting phage PO4 selects for mutations in a variety of T4aP genes

Phage PO4 is a lytic phiKMV-like T4P-targeting phage that infects *P. aeruginosa* strain PAO1 (7). We used PAO1 for these studies because it lacks a functional CRISPR system, therefore it relies on resistance mechanisms that act at other steps of phage infection, such as receptor recognition. Following co-culture of PAO1 with PO4, 128 PO4-resistant colonies of *P. aeruginosa* were recovered. None of the phage-resistant mutants (PRMs) twitched in a standard agar sub-surface assay (**Supplementary Figure S2**) suggesting that these strains had non-functional T4aP (3, 27).

Whole genome sequencing followed by breseq analysis was used to identify relevant mutations. Among the 128 PRMs, we identified 28 unique mutations spanning 16 different pilus-related genes (**Figure 1 and Table 1**), suggesting that some mutants were clonal. Seventeen mutations resulted in truncation of the gene product and predicted loss of the protein. The remainder were small indels or single nucleotide polymorphisms (SNPs) predicted to alter protein function without disrupting expression. Most mutations affected only single genes, but one PRM had a large 7559-base deletion that spanned *pilS-pilY1*, removing a region that includes most of the minor pilin operon, plus the *pilSR* genes encoding a two-component system (TCS) that regulates PilA expression (39). Mutations spanned all the T4P structural subcomplexes

133 (pilus, motor, alignment and secretin) plus PilS-PilR. Multiple non-clonal mutations in some
134 genes were identified, including *pilM* (4 different PRMs), 3 in *pilB*, 3 in *pilR*, and 2 in each of
135 *pilA*, *pilC*, *pilD*, and *pilQ*. There was no correlation between the size of the gene and the number
136 of unique mutations identified. For example, only one mutation in *pilY1* (3486 bp) was recovered
137 even though it is nearly double the length of *pilB,* in which multiple mutations were identified.
138 Intriguingly, in four of the PRMs we could identify no mutations, despite repeated sequencing,
139 pooling of the sequence data, and careful analysis of read depth (below). These strains remained
140 phage insensitive after passage, suggesting they are stably resistant descendants of the PAO1
141 parent strain.

142 While complete loss of a gene product may result in an expected phenotype, SNPs and
143 indels in the PRMs could generate informative intermediate phenotypes. Therefore, the levels of
144 intracellular and extracellular pilins were assessed to test whether the mutations we identified
145 resulted in loss of pilin expression and/or pilus assembly. Most PO4 PRMs expressed the major
146 pilin subunit PilA at wild-type levels in whole cells, but failed to produce extracellular pili
147 **(Supplementary Figure S2**). These data indicated that phage resistance in these PRMs results
148 from impaired function of the pilus assembly machinery (**Table 1, Supplementary Figure S2**).

149 We identified three PRMs with recoverable extracellular pili, despite their lack of motility
150 **(Figure 2)**. One of these had a 4-base deletion (residues 568-571) in *pilT* encoding the retraction
151 ATPase that caused a frameshift leading to a premature stop codon. *pilT* mutants produce
152 extracellular pili, but PilT-mediated pilus retraction is required for PO4 susceptibility. Thus, loss
153 of this protein is consistent with previously reported phage susceptibility patterns (18). The other
154 two mutations were in the extension ATPase PilB and the prepilin peptidase/methyltransferase
155 PilD. Since mutations in those proteins have not been reported to confer phage resistance while
156 maintaining pilus expression, we examined them more closely.

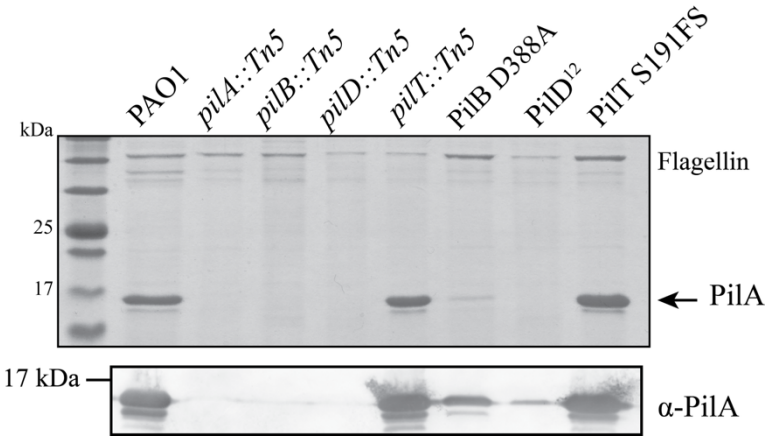

157

158 **Figure 2. Phage-resistant mutants with lesions in PilB, PilD, or PilT still had recoverable surface**
159 **pili.** Sheared surface protein samples separated on 15% Coomassie-stained SDS-PA gel (top) and Western
160 immunoblot using α-PilA antisera (bottom) of sheared surface protein samples show pilins can be
161 recovered in these phage resistant mutants. Blot is representative of three independent experiments.

162 **PilB D388A confers phage resistance without loss of pilus extension**

163 The assembly ATPase PilB is a member of the Additional Strand Catalytic 'E'
164 superfamily (40). Its Walker B motif (residues D390-E396) coordinates a Mg^{2+} required for ATP
165 hydrolysis (40–42), and this activity is essential for pilus assembly. We identified a PilB D388A

166 mutation adjacent to the Walker B motif. Western blotting of whole cell lysates with a polyclonal
167 PilB antibody showed that PilB D388A was expressed at levels similar to wild type (**Figure 3A**)
168 suggesting the mutation does not affect protein stability, even though the mutant had fewer
169 recoverable surface pili than wild type (**Figure 2, Supplementary Figure S1**). To test whether
170 PilB D388A confers resistance to other T4P-targeting phages, the mutant was challenged with
171 broad host range temperate phage DMS3 (43) and JBD68, which uses a minor pilin as its
172 receptor (44) (**Figure 3B**). The PRM was resistant to both those T4P phages.

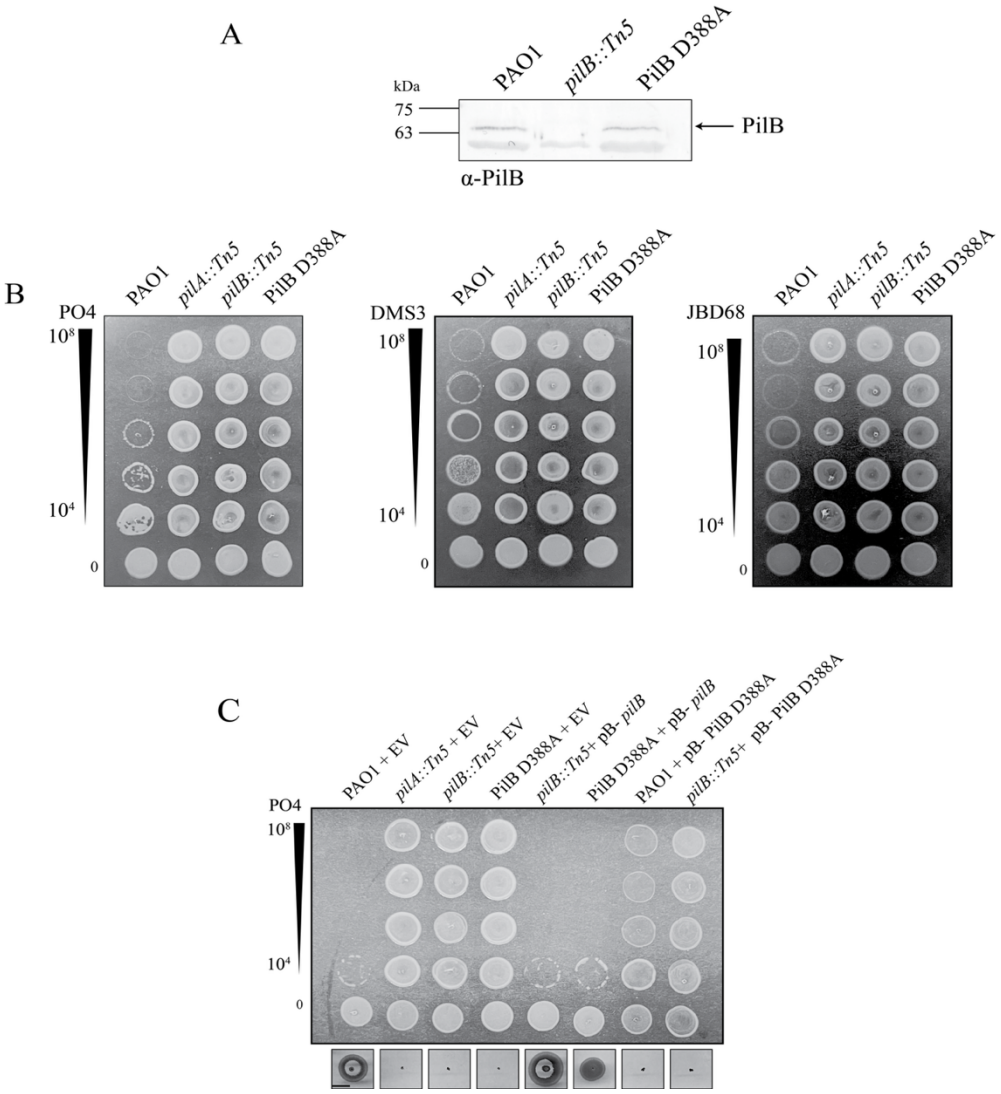

173 **Figure 3. PilB D388A is stable and confers resistance to multiple T4P-targeting phages. A)** Western
174 immunoblot of whole cell lysates using α-PilB antisera showed that PilB D388A levels are comparable to
175 wild-type PilB. Blot is representative of three independent experiments. **B)** PilB D338A is resistant to
176 three different T4P-targeting phages. Serially diluted phages PO4, DMS3, and JBD68 were combined
177 with standardized bacteria liquid cultures were spotted on 0.6% LB agar. Phage titres (PFU) are indicated
178 to the left. **C)** Overexpression of *pilB in trans* in PilB D388A rescues phage susceptibility and twitching
179 motility. Complementation of PAO1 or a *pilB::Tn5* mutant with PilB D388A abolishes twitching motility
180 and phage susceptibility. Samples were induced using 0.2% L-arabinose. Scale bar indicates 1 cm. EV=
181 empy vector, pB= pBADGr. Images are representative of three independent experiments.

182 Since PilB functions as a homohexamer (40), we tested for possible dominant-negative
183 effects of expressing the mutant allele *in trans*. When wild-type PilB was expressed from a
184 plasmid in PilB D388A, phage susceptibility and twitching motility were recovered, although
185 motility was approximately 75% of wild-type (**Figure 3C**). In the reciprocal experiment,
186 expression of PilB D388A from a multicopy plasmid in the wild type abolished twitching
187 motility and phage susceptibility (**Figure 3C).** Similarly, complementing PilB-deficient strains
188 with PilB D388A failed to restore twitching motility or phage susceptibility (**Figure 3C**),
189 providing further evidence that this mutation impairs pilus function.

190 **A partial PilD duplication delays pilin maturation to confer phage resistance**

191 The third PRM with recoverable surface pili had a 12-base duplication in *pilD* **(**PilD^{12};
192 **Table 1, Figure 2)**. PilD is a membrane-embedded bifunctional prepilin peptidase that cleaves
193 the type III signal sequence of both T4P pilins and type II secretion system (T2SS) endopilins,
194 and methylates the first residue of the mature (endo)pilins (14, 45–47). The duplication added
195 four residues (duplication of F184-V187) to a helix that is distal to the predicted peptidase and
196 methyltransferase active sites (**Figure 4A**). PRMs with this mutation had few recoverable
197 extracellular pili that were not visible on SDS-PAGE, although they could be detected on
198 Western blots **(Figure 2),** and did not twitch (**Supplementary Figure S2**).

199 To more easily monitor the impact of this mutation on PilD peptidase function, we
200 replaced the native 6-residue signal sequence of PilA with the 18-residue signal sequence of
201 HxcT, the major endopilin of the Hxc T2SS in *P. aeruginosa* and also a substrate of PilD (48),
202 creating a chimeric pilin, PilA^{chimera} (**Figure 4B).** Replacement with a longer signal sequence
203 allowed for better resolution of the change in mass of the chimera following cleavage compared
204 to wild-type PilA. Whole cell Western blot of chimeric pilins in PilD^{12} at 6- and 8- hours post
205 subculture revealed a mixture of processed and unprocessed subunits, while the wild-type control
206 had only processed subunits (**Figure 4C**). By 16-hours post subculture, all pilins were processed
207 (**Figure 4C**). These data suggested that PilD^{12} cleaves prepilins less efficiently than its wild-type
208 counterpart. Since PilD also processes the endopilins of the T2SS, we assessed protease secretion
209 of PilD^{12}. The mutants had no visible zone of clearing on skim milk plates even after 24 hours of
210 incubation, suggesting impaired T2SS activity and supporting the hypothesis that PilD function
211 was impaired (**Supplementary Figure S5**).

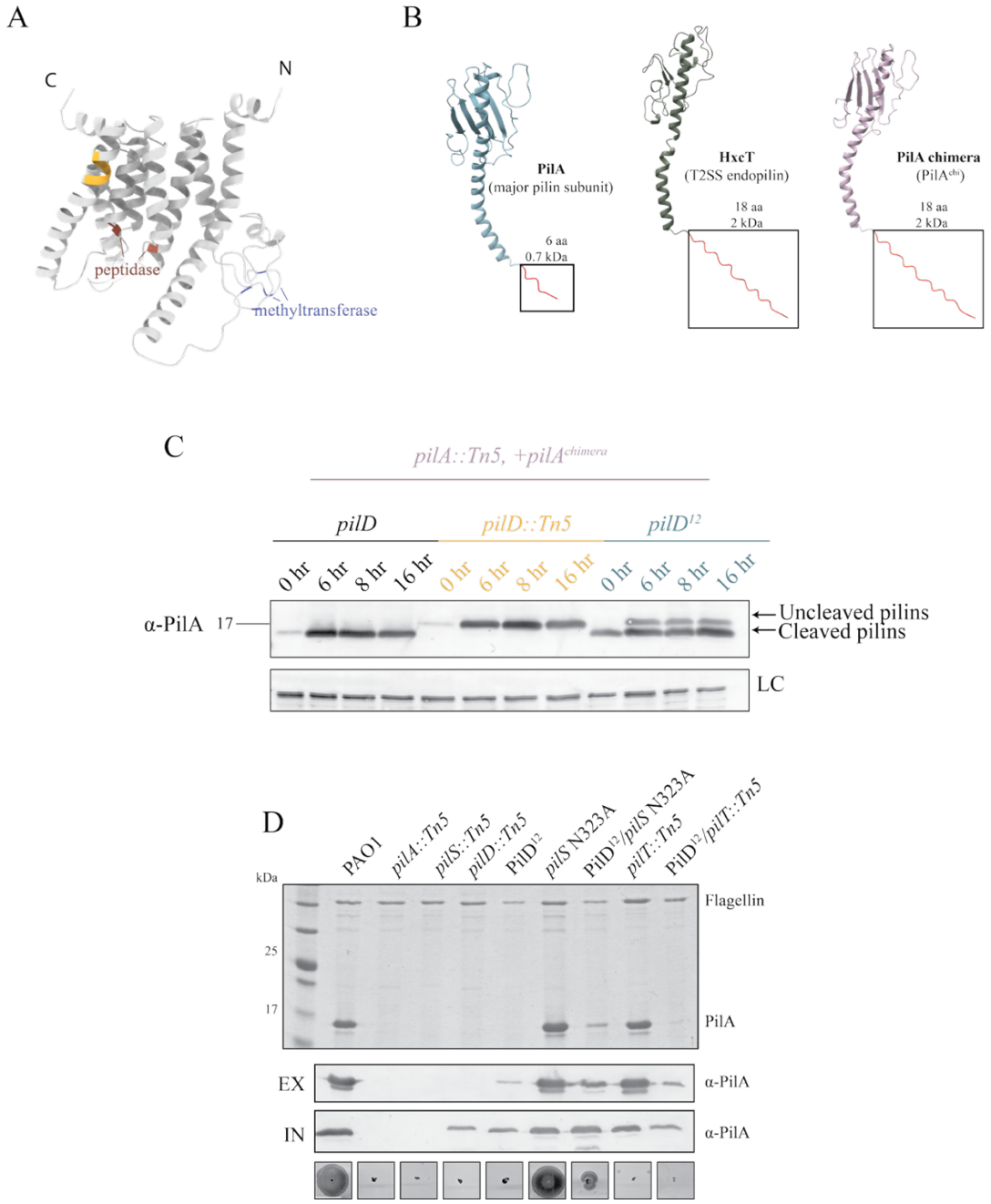

Figure 4. PilD^{12} mutants have reduced T4P expression and function. A) AlphaFold3 PilD^{12} structural model (confidence data available in **Supplementary Figure S3)**, with the 4-amino acid insertion highlighted in yellow. Key peptidase active site residues (D149, D217) are shown in blue, predicted methyltransferase residues (C72, C75, C97, C100) in purple (UCSF Chimera X). **B)** Models of PilA and the endopilin HxcT, with the leader sequences highlighted in red. Structures were predicted using AlphaFold3 **(**confidence data in **Supplementary Figure S2)** and modeled using UCSF Chimera X. The lengths and molecular weight of the leader sequences are indicated. The leader sequence of PilA was replaced with the HxcT leader sequence to create PilA^{chimera}. **C)** In *pilD^{12}*, intracellular pilins are a mixed population of cleaved and uncleaved at 6- and 8- hr post subculture, while only cleaved pilins were detected in wild type. Pilins at 16 hr were mostly cleaved. Samples were induced using 0.2% L-arabinose and separated on 16% Tris-Tricine gels followed by Western immunoblot analysis using α-PilA antisera.

224 Blot is representative of three independent experiments. **D)** *pilD*^{12} has fewer recoverable surface pili than
225 wild type, but introduction of the feedback-insensitive PilS N323A allele increases recoverable surface
226 pili. Sheared surface protein samples were separated on 15% Coomassie-stained SDS-PA gel (top).
227 Western immunoblot using α-PilA antisera of cell lysates (bottom) shows the levels of intracellular pilins
228 relative to controls. Data are representative of three independent experiments. Twitching motility of
229 PilD^{12} and mutants correlate with the amount of recoverable pili. Scale bar indicates 1cm.
230 IN=intracellular, EX= extracellular, EV= empty vector, pB= pBADGr.

231

232 Unprocessed pilins cannot be assembled, so they accumulate in the cytoplasmic
233 membrane where they act as regulatory ligands to suppress the further expression of PilA via
234 their interaction with the sensor kinase, PilS (39). Thus, the PilD^{12} mutation has the potential to
235 reduce pilin availability in two ways: slowing pilin maturation and inhibiting expression of new
236 prepilins due to the resulting backlog of unprocessed subunits. To test if this potential bottleneck
237 could be alleviated by increasing the amount of prepilins produced, we introduced a PilS N323A
238 point mutation into the *pilD*^{12} background. PilS N323A lacks the ability to dephosphorylate the
239 response regulator PilR when PilA accumulates, allowing *pilA* expression to continue (39). PilS
240 N323A/*pilD*^{12} had fewer recoverable extracellular pilins and less twitching motility than WT
241 (**Figure 4D)**, but more surface pili than the control strain, retraction-deficient PAO1
242 *pilT::Tn5/pilD*^{12} (**Figure 4D)**. In *pilT* backgrounds, surface piliation is maximal since any pili
243 that can be assembled are trapped on the surface due to loss of the retraction ATPase. Low
244 surface pili levels in PAO1 *pilT::Tn5/pilD* suggests that there is a pilus assembly defect in PilD^{12}
245 strains that can be partially rescued through PilR hyperactivity.

246 Because introduction of PilS N323A restored twitching motility, we next evaluated if
247 phage susceptibility was also rescued. PilS N323A is predicted to increase pilin production, so as
248 an additional control we tried expressing *pilA* from an arabinose-inducible promoter in the *pilD*^{12}
249 background. PO4 susceptibility was assessed in a co-culture assay, where phages and bacteria
250 were mixed and spotted onto agar. PilS N323A/*pilD*^{12} was susceptible to PO4 killing, but
251 unexpectedly, *pilA* overexpression *in trans* in *pilD*^{12} did not restore PO4 susceptibility **(Figure**
252 **5A)**. Similarly, in a standard plaque assay, PilS N323A/*pilD*^{12} was susceptible to PO4 and two
253 other T4P-targeting phages while PilD^{12} + pBADGR-*pilA* was resistant (**Figure 5B)**.
254 Interestingly, a faint plaque was observed for both PilD^{12} and PilD^{12} + pBADGR-*pilA* strains at
255 the highest DMS3 titre tested, showing that both strains may be modestly susceptible to that
256 phage (**Figure 5B)**. Introduction of PilS N323A or overexpression of *pilA* from an arabinose-
257 inducible promoter increased twitching motility in the *pilD*^{12} background, although not to wild
258 type levels **(Figure 5C)**. These data suggest that the lack of twitching motility and decreased
259 surface piliation in PilD^{12} is due to a combination of decreased pilin processing and negative
260 feedback from accumulation of unprocessed pilins in the inner membrane. Both overexpression
261 of *pilA* and PilR hyperactivity increased prepilin production and restored twitching motility in
262 PilD^{12} but for reasons that are not yet clear, these strategies had different effects on phage
263 susceptibility.

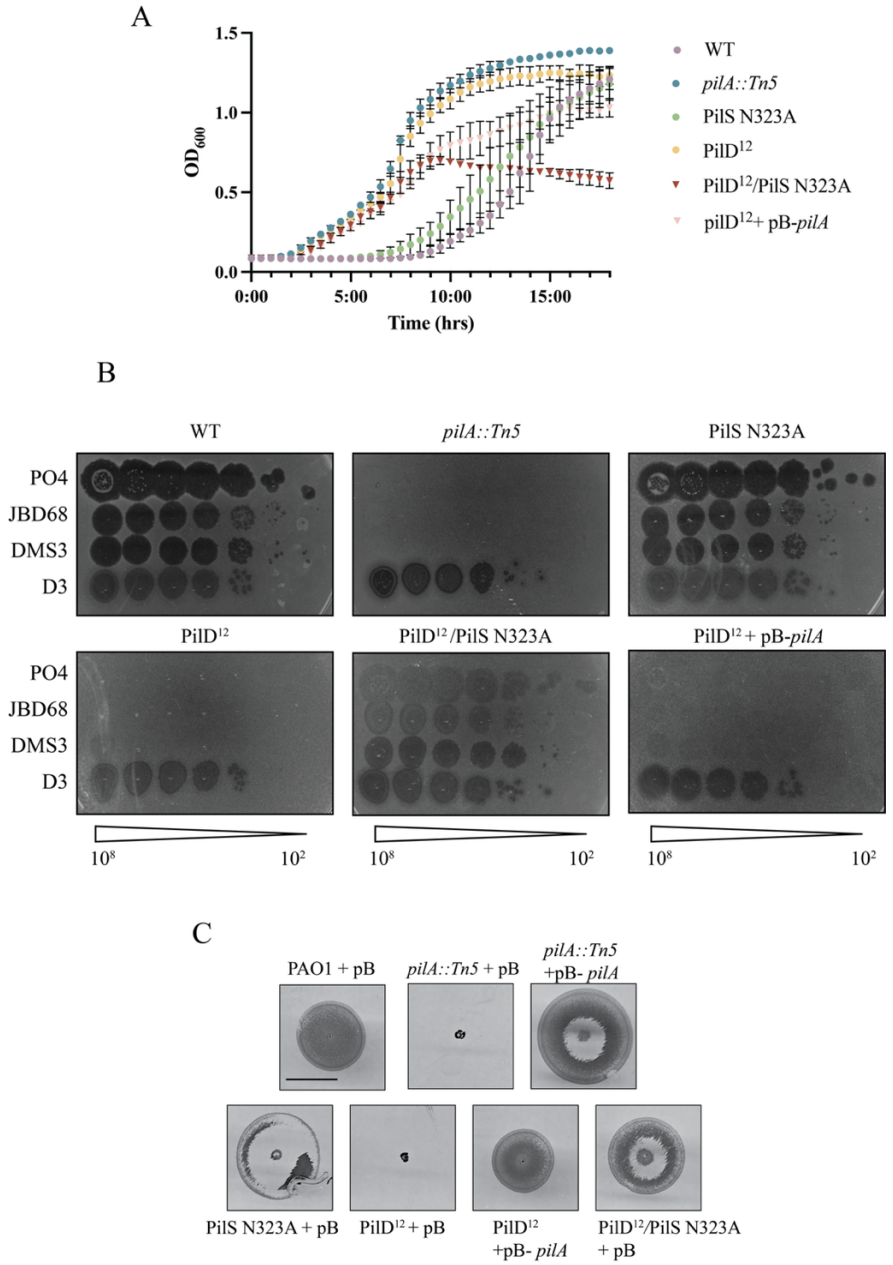

Figure 5. PilS N323A restores both twitching motility and phage susceptibility in PilD^{12} strains while overexpression of *pilA in trans* restores only motility. A) PilD^{12}/PilS N323A is susceptible to PO4 while PilD^{12} + pBADGR- *pilA* is resistant in a liquid co-culture phage killing assay **B)** PilD^{12}/PilS N323A is susceptible to 2 other T4P targeting phages while PilD^{12}+ pBADGR- *pilA* is partly susceptible only to DMS3. D3 is a LPS-specific phage control. Phage titres (PFU) are indicated below each set of plaque assays. C**)** Twitching motility, but not PO4 susceptibility, was recovered by overexpression of *pilA in trans* in PAO1 *pilD^{12}*. Samples were induced using 0.2% L-arabinose. Scale bar indicates 1 cm. Images are representative of three independent experiments. pB= pBADGr.

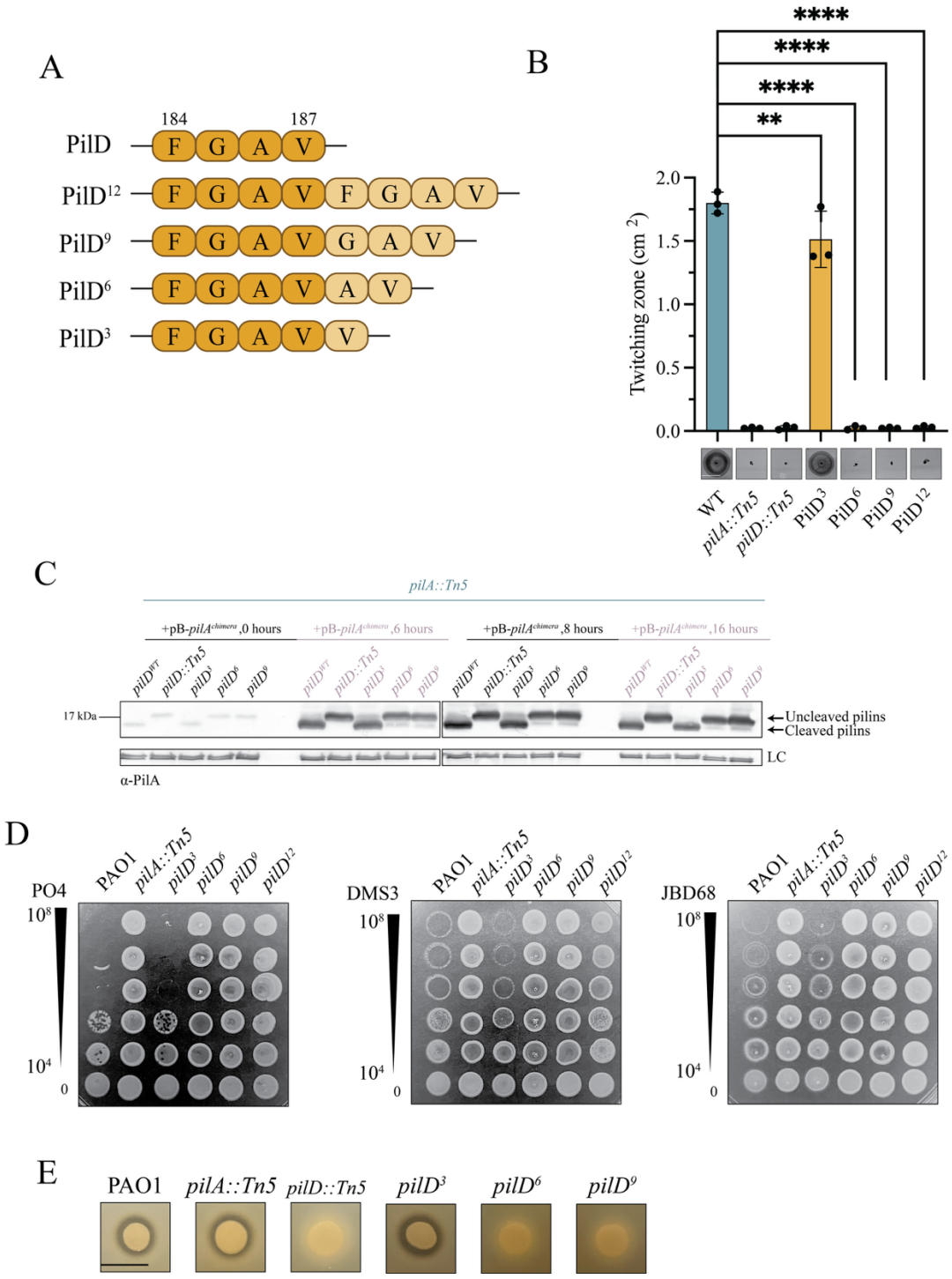

Figure 6. A two- or three-residue insertion at PilD V187 disrupts pilin processing. A) Schematic of PilD mutants. Lighter coloured residues are additions relative to wild-type residues. **B)** PilD^3 twitches while other strains do not. Twitching zone measurements are an average of three independent experiments containing three replicates each. Twitching images are representative of three independent experiments. Scalebar represents 1cm. ** p=0.008, ****p<0.001. **C)** PilD^6 and PilD^9 peptidase activity is impaired as intracellular pilins were uncleaved at all time points, while PilD^3 is functional. Samples were loaded on 17% Tris-Tricine gels followed by Western immunoblot analysis using α-PilA antisera. Flagellin levels

were used as loading control. Blot is representative of three independent experiments. Samples were induced using 0.2% L-arabinose. **D)** PilD^{3} is susceptible to T4P-targeting phages while PilD^{6} and PilD^{9} are resistant. Bacteriophage plaque assays were performed using serially diluted stocks of phages PO4, DMS3, and JBD68. Titres (PFU) are indicated to the left. Image is representative of three independent experiments. **E)** *pilD^{3}* spotted on a skim-milk agar plate had a visible zone of clearance, indicating protease secretion. No zone is visible in *pilD^{6}* and *pilD^{9}* suggesting impaired T2SS function. Scale bar represents 1cm. Samples are representative of three independent experiments.

To determine if changing the size of the PilD insertion impacted function, we created three additional mutants with one, two, or three amino acids inserted (PilD^{3}, PilD^{6}, and PilD^{9}) (**Figure 6A**). PilD^{3} twitched ~85% (p=0.008) of WT, while PilD^{6} and PilD^{9} lacked twitching motility (**Figure 6B**). Intracellular pilins from PilD^{3} were processed, while those from PilD^{6} and PilD^{9} were unprocessed at all timepoints (**Figure 6C**), consistent with their non-twitching phenotypes. PilD^{3} phage susceptibility was comparable to that of wild-type PAO1, while PilD^{6} and PilD^{9} were resistant to all three phages tested **(Figure 6D).** T2SS activity was maintained in PilD^{3} but not PilD^{6} and PilD^{9} (**Figure 6E**). Therefore, only one or four residues can be inserted at V187 in PilD while maintaining at least partial function.

Only mutants with sequence duplications readily regain pilus function

For clinical applications, it is important that phage-resistant strains do not regain pathogenicity after treatment has ended, as this could contribute to recurrence of infection. Therefore, we evaluated if the PRMs recovered here could regain twitching motility, a key virulence trait, in the absence of phage pressure. Four representatives of the types of mutations that were commonly recovered in our screen were randomly selected for analysis. These included *pilT* Δ568-571 (deletion), *pilQ* C1282T (nonsense mutation), *pilB* A832C (point mutation), and PilD^{12} (duplication). Each of the mutants were first tagged with a gentamicin resistance gene as described in the Methods to ensure that any twitching colonies recovered were descendants of the relevant strains. Ten colonies of each mutant were stab-inoculated into standard 1% LB twitching agar plates. After a week of incubation at room temperature, only PilD^{12} colonies yielded twitching revertants (**Figure 7A**). When repeated with larger numbers, almost half of PilD^{12} colonies (45%, n=100) regained twitching motility. Since second-site suppressor mutations are more likely to occur in bacteria versus reversion to wild-type sequences (49), the *pilD* gene was sequenced. All sequenced twitching colonies had wild-type *pilD* sequences. As a control, we generated a PilD^{12} variant (PilD^{12Var}) with the same 4 amino acids inserted but using different codons (**Figure 7B**). None of the PilD^{12Var} colonies tested regained twitching motility following a similar week-long incubation (**Figure 7C).** These data suggest that reversion in *pilD^{12}* was likely facilitated by slipped strand mispairing that resolved the original duplication event (50).

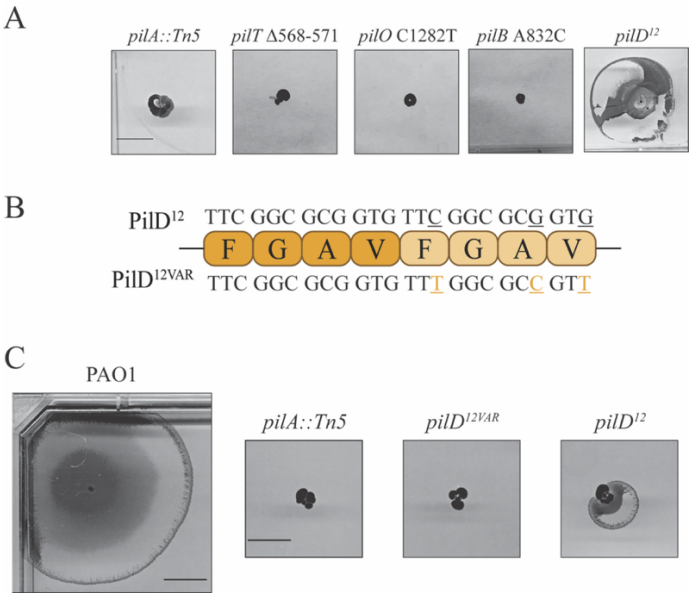

Figure 7. Only strains with sequence duplications readily regain motility. A) Randomly selected PRMs representative of each form of mutation isolated in our initial screen underwent a seven-day twitching assay, and only PilD^{12} regained motility. **B)** Schematic of PilD ^{12VAR} mutant. Lighter residues are additions relative to wild-type residues (in dark). Bases are indicated above and below amino acids with altered bases underlined in orange. **C)** PilD^{12} and PilD^{12VAR} underwent a seven-day twitching assay. Images are representative of three independent experiments. Scale bar represents 1 cm.

A subset of resistant non-twitching strains had no identifiable mutations

Of the 128 individual PRM colonies selected, eight initially had no detectable genomic variants supported by our defined cutoff of >50 reads, which is considered sufficient for mutation identification (51, 52). Since they were not 'mutants' in the traditional sense, we called these isolates 'resistant and non-twitching strains' (RANTS). In phenotypic analyses, three RANTS expressed no pilins, three had no recoverable surface pili but produced pilins intracellularly, and two expressed surface pili (**Supplementary Figure S2)**. These data suggested that the RANTS were not clonal. All RANTS were resistant to the other T4aP-targeting phages, DMS3 and JBD68 (**Figure 8A).**

To rule out technical errors, three randomly selected RANTS were re-sequenced and analyzed, plus those second-round sequences were concatenated with the first-round sequences to increase the read depth. Despite this increased sequence coverage, we still could identify no mutations above our cutoffs. While breseq uses a conservative, binary approach to identify mutations such as SNPs and indels, it completes a secondary analysis that considers intermediate mutations, those that do not pass the binary cutoff but where the sequence varies from the reference, to account for mixed genomic populations or potential sequencing issues (53–55). Mutations identified using this secondary form of analysis are classified as "marginal" mutations. Using this secondary analysis, relevant mutations could be mapped to four of the eight RANTS **(Table 2)**.

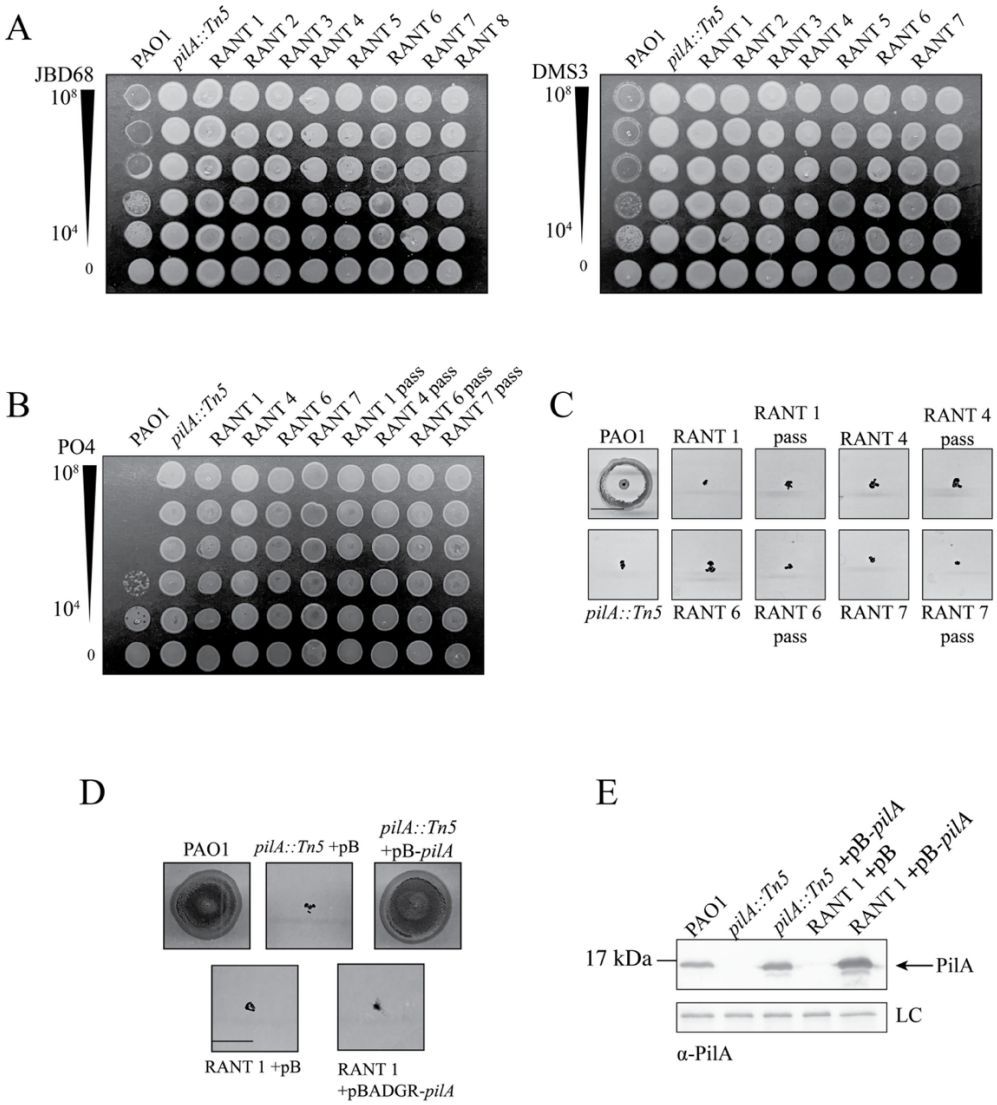

Figure 8. RANTS are resistant to other T4P-targeting phages and phenotypes are stable following passage in phage-free media. A) All RANTS are also resistant to T4P-target phages DMS3 and JBD68. Bacteriophage plaque assays using serially diluted stocks of phages PO4, DMS3, and JBD68. Titres (PFU) are indicated to the left. **B)** Following 14-day passaging in phage free nutrient-rich media, passaged RANTs (denoted with "pass") maintained PO4 resistance and **C)** lack of twitching motility. **D)** Overexpression of *pilA in trans* in RANT 1 failed to restore twitching motility, suggesting that it has additional defects besides lack of pilin expression. Scale bar represents 1cm. **E)** Western immunoblot analysis of *pilA* expression using α-PilA antisera was used to confirm *in trans* expression**.** Samples were induced using 0.2% L-arabinose. Samples are representative of three independent experiments.

To assess the stability of resistance in the remaining RANTs, they were passaged daily in phage-free LB media. After 14 days of passage, all remained PO4-resistant and non-twitching (**Figure 8B, 8C**), suggesting that the phenotypes are stable in the absence of phage pressure. As a final confirmation of sequencing quality, *pilA, pilS,* and *pilR* were sequenced in the RANTs that did not produce pilins, as these genes contribute to PilA production. All had wild-type sequences, confirming that mutations in those genes were not responsible for phage resistance. Finally, we

363 tested whether the resistant phenotype of RANT1, which did not produce detectable pilins, could
364 be rescued by *pilA* expressed *in trans*. Neither pilus function nor phage susceptibility was
365 restored in the RANT1 background (**Figure 8D**) even though pilins were successfully expressed
366 from the plasmid (**Figure 8E**), suggesting that both pilin expression and pilus assembly were
367 perturbed in that strain.

368

369 **DISCUSSION**

370 LPS and T4P are the most common phage receptors for *P. aeruginosa* (56–58), and most
371 therapeutic cocktails include phages that recognize those surface structures. Here, we evaluated
372 the repertoire and stability of mutations conferring resistance to a lytic T4P-targeting phage,
373 PO4. This phiKZ-like phage has been used as a reporter of *P. aeruginosa* pilus function for
374 decades and was originally used to identify putative genes involved in T4P biogenesis (18, 25,
375 59). Although initially reported to be specific for the PAK strain (7), our stock can infect PAO1
376 as well as PAK. We found mutations conferring PO4 resistance in genes encoding most structural
377 components of the T4P, plus the PilSR TCS, and all resulted in loss of twitching motility. No
378 hypothetical or unannotated genes associated with phage resistance and/or loss of twitching
379 motility were identified in our analysis of this well-characterized strain. With the exception of
380 PilD[12], the subset of mutants we tested remained stably resistant over one week of growth in the
381 absence of phages. A limitation of this study is use of non-selective growth conditions, where
382 loss of T4P does not impose a fitness cost. In the more complex environment of the host,
383 selection of suppressors that maintain fitness may be more likely.

384 In addition to revealing how bacteria can become resistant to phages, the serendipitous
385 mutations that are selected can provide new insights on the roles of pilus machinery components
386 and the residues that are key for their function. It seems unlikely that there are genetic "hot
387 spots" for mutations that confer resistance to T4P-targeting phages given the distribution of
388 mutations we found in a variety of genes. Genomic factors such as operon order, role of the
389 protein, size and sequence of the gene, and additional factors such as effects on fitness may
390 contribute to likelihood of mutation selection. Although we looked for them, we found no phage-
391 resistant mutants that retained the ability to twitch, suggesting that loss of pilus function or
392 expression is by far the most likely route to resistance.

393 At least 40 genes are directly or indirectly involved in *P. aeruginosa* T4P function and
394 regulation (3, 11). We identified mutations in 16 unique genes, encoding members of the T4P
395 alignment subcomplex, PilD, the PilSR TCS, some minor pilins, and two out of three ATPases.
396 Most of the genes identified encode structural or enzymatic components, and of those, *pilD* is the
397 only one shared with another system, the T2SS (47). When considering which pilus genes were
398 not found in our screen, it is important to note that mutation of only a subset of known pilus
399 genes is expected to result in phage resistance and/or loss of twitching motility. For example, the
400 auxiliary retraction ATPase PilU is required for twitching motility but not phage infection,
401 showing that the phenotypes can be separated (18). Components of the regulatory Pil-Chp
402 chemotaxis system that increases intracellular cAMP levels in response to pilus surface sensing
403 were not identified in our screen (60). However, a mutation in the Pil-Chp chemoreceptor PilJ
404 was reported in PRMs resistant to another T4P-targeting phage (61). *pilJ* mutants have low levels
405 of cAMP and thus reduced expression of surface pili, which could impact their susceptibility to
406 phages that are sensitive to receptor abundance (62, 63). Most mutations we identified were

407 SNPs or small indels, though some large genomic deletions were also identified. These patterns
408 are comparable to those in other studies that reported mutations in *P. aeruginosa* PRMs (37, 61,
409 64, 65).

410 Three PRMs identified here had mutations in *pilB,* a frequently reported hit in other
411 studies of phage-resistant mutants (37, 61, 64, 65). Interestingly, one of the PilB mutations
412 identified here, PilB T278P, was also reported in PRMs isolated by another group, using a
413 different phage (65). The other PilB mutation we identified, PilB D388A, is adjacent to the
414 Walker B motif and the mutant produced reduced levels of surface pili that did not support
415 motility (**Figure 2)**. While D388 is not directly involved in Mg^{2+} coordination, this mutation may
416 lead to structural changes in PilB that indirectly affects its ATPase activity, reducing pilus
417 assembly. A previously described point mutation (E354Q) in a conserved residue of the Asp Box
418 involved in Mg^{2+} coordination, also important for ATPase activity, resulted in reduced twitching
419 motility (66). Phage susceptibility of this mutant was not assessed. These examples suggest that
420 mutations that reduce but do not abolish PilB function are sufficient to decrease pilus assembly,
421 potentially leading to phage resistance. It is also notable that PilB and its regulatory partners such
422 as PilZ are favoured targets of various prophage-encoded inhibitory proteins that impair pilus
423 function to provide super-infection exclusion (67, 68). PilB may be a common prophage target
424 because pilus extension is energetically costly, with each pilin incorporation event requiring two
425 molecules of ATP (40). Therefore, inhibition of PilB activity may improve growth and fitness of
426 the lysogen. Mutations in *pilB* have been identified in clinical isolates, both independent of and
427 following phage therapy (69, 70). Although the specific mutations are not always defined, these
428 data suggests that such strains can survive *in vivo.*

429 We also recovered a PRM with a 12-base duplication in *pilD*. We showed that $PilD^{12}$ has
430 impaired pilin processing, with mixed populations of mature and uncleaved pilins at 6- and 8-
431 hours post induction. The $PilD^{12}$ uninduced overnight samples (0 hr) **(Figure 4D)** had more
432 pilins than the WT *pilD* and *pilD::Tn5* uninduced overnight samples. This reproducible
433 phenotype **(Supplementary Figure S4)** suggests that $PilD^{12}$ may increase pilin inner-membrane
434 levels. We hypothesize that the reduced processing capacity of $PilD^{12}$ limits the number of
435 mature pilins available for incorporation into the growing pilus and thus fewer surface-exposed
436 pili. Simultaneously, the prepilins that accumulate repress further PilA expression via their
437 interactions with the PilSR system (**Figure 9A**). Together, these events lead to a pronounced
438 decrease in availability of mature pilins for pilus incorporation. Combining a PilS N323A
439 mutation with $PilD^{12}$ addressed these issues by increasing the overall amount of prepilins
440 (**Figure 9B)**, restoring motility and phage susceptibility (**Figure 4D)**. However, expressing PilA
441 from a plasmid, which also increases overall amount of prepillins, restored twitching motility but
442 not phage susceptibility **(Figure 5)**. In PilS N323A, PilR is locked in its phosphorylated, active
443 state; in contrast, overexpression of PilA from a plasmid leads to PilR dephosphorylation by PilS.
444 Our data suggest that increasing pilin abundance in $PilD^{12}$ is sufficient to restore twitching
445 motility, but successful phage replication may also require PilR activation. In addition to *pilA*,
446 PilR regulates a large set of genes including those encoding the minor pilin subcomplex and
447 PilBCD (71). Increasing pilin production through the PilSR TCS coordinately upregulates other
448 pilus genes to produce more pili that phages can recognize. Phage replication is also affected by
449 cell metabolism and growth (72, 73). PilR also regulates a subset of host metabolic enzymes that
450 may similarly contribute to phage replication (71).

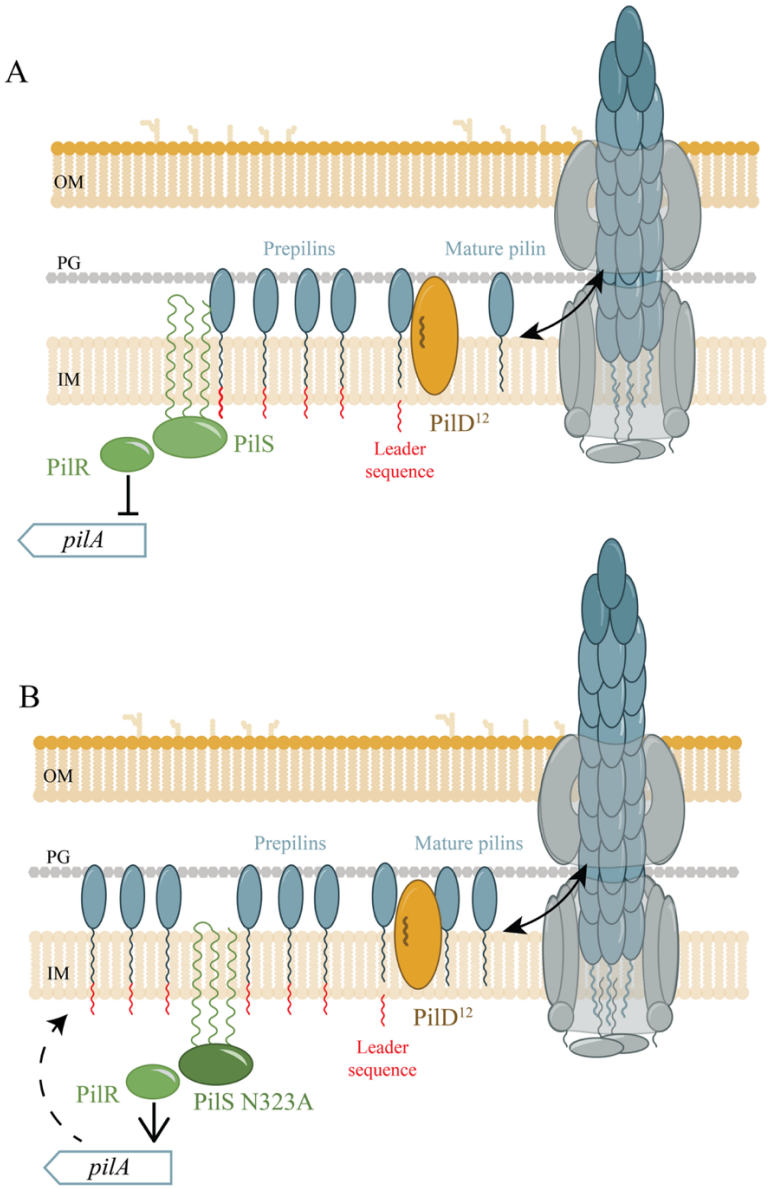

Figure 9. Model of PilS-dependent alleviation of the PilD^{12} decrease in pilus assembly. A) In PilD^{12} background, accumulation of prepilins in the inner membrane is sensed by PilS which dephosphorylates PilR, decreasing *pilA* expression. This results in production of fewer pre-pilins, further reducing the pool of mature pilins that can be assembled into pili. **B)** In PilS N323A, feedback inhibition by prepilins is lost and phospho-PilR continues to promote *pilA* expression, increasing the total pool of prepilins. This allows for more pilins to be processed by PilD^{12}, increasing pilus assembly.

Based on structural predictions, the PilD^{12} duplication is located in the fifth transmembrane helix of PilD, distal from the cytoplasm-facing peptidase and methyltransferase active sites **(Figure 4A).** One complete turn of an α-helix requires ~4 amino acids to maintain correct hydrogen bonding (74). Inserting two or three residues in PilD^{6} and PilD^{9}, respectively,

463 likely disrupts hydrogen bonding, affecting protein stability or its interaction with pilins. Those
464 two mutants resembled a strain lacking PilD in terms of phage susceptibility, motility, and
465 secretion. In contrast, PilD[12] is predicted to lengthen the helix by one complete turn, allowing the
466 enzyme to retain partial function. Despite its essential role in function of the T4P and T2SS
467 systems and contributions to *P. aeruginosa* virulence, PilD has been poorly characterized
468 compared to other components (75). This interesting mutation provides new insight into
469 allosteric control of PilD's peptidase function.

470 We were surprised to isolate some strains that were stably phage-resistant and non-
471 twitching (RANTs) where we could identify no mutations. Some were ultimately resolved by
472 further scrutiny of mutations that did not pass the initial sequence quality and read depth cutoffs,
473 but there were still 4 RANTS with genomes that appeared identical to their WT parent strain.
474 The ability of *P. aeruginosa* to become phage resistant in the absence of obvious mutations has
475 been reported previously (76, 77). It is possible that epigenetic changes following phage
476 exposure could result in silencing of key genes (i.e. pilus structural components, genes that
477 directly or indirectly regulate T4P function, or combinations thereof) . In *Ralstonia*
478 *pseudosolanacaerum*, methylation patterns that arose during growth in the plant host persisted
479 for up to 22 passages outside of the host, demonstrating the longevity of prokaryotic epigenetic
480 modifications (78). Such changes might be detected using newer forms of whole genome
481 sequencing such as PacBio or Oxford Nanopore sequencing (79, 80). Thus, future work using
482 these more advanced sequencing technologies may shed light on how phage resistance can be
483 achieved in the absence of detectable mutations.

484 The inexorable rise of antibiotic resistance has led clinicians to reconsider phage therapy
485 as an option (81). Most published case studies show that it is successful and safe, supporting this
486 approach (82, 83). Our findings can inform development of phage therapy and phage steering
487 strategies. One caveat of this work is that PRMs were selected in rich media, and more host-like
488 conditions (eg. nutrient limitation, immune system components) might affect the types of
489 mutations that are selected. However, phage resistance patterns identified *in vitro* appear to
490 accurately reflect those arising *in vivo* (70).

491 Our data suggest that T4P-targeting phages mostly select for mutations causing the
492 irreversible loss of a key virulence factor. Strains lacking T4P have decreased pathogenicity in
493 different *in vivo* models (58, 84–86), therefore this phenotype may be clinically beneficial.
494 Ideally, T4P-targeting phages should be combined with phages using other receptors, such as
495 LPS, to address resistance and emergence of potential revertants. This strategy has been applied
496 in phage cocktails BFC1 and 2, created by the Queen Astrid Military Hospital in Belgium. Both
497 contain T4P-targeting phage PNM, along with a LPS-targeting phage and other phage(s) with
498 unknown targets (87–89). These cocktails as well as PNM alone have been successful in
499 clearance of infection (83).

500 T4P are common surface structures that are expressed by other important human
501 pathogens, including *Acinetobacter baumannii*, *Stenotrophomonas maltophilia, Neisseria*
502 *meningitidis, Streptococcus pneumoniae,* and *Clostridioides difficile* (2, 90–92). Pilus-targeting
503 phages for many of these pathogens have been identified (8, 93). Similarly, plant pathogens
504 *Xylella fastidiosa, Xanthomonas axonopodis, Xa. euvesicatoria,* and *P. syringae* express T4P, and
505 pilus-targeting phages have been identified for those species as well (94, 95). The use of phages
506 in agriculture for biocontrol is a growing field (96, 97). It will be interesting to learn whether

507 T4P-targeting phages for other host species will select for similar repertoires of escape
508 mutations.

509

510 **METHODS**

511 **Bacterial strains and growth conditions**

512 Bacterial strains were grown in lysogeny broth (LB) at 37°C with shaking (200 rpm) or
513 on 1.5% agar plates supplemented with antibiotics with the following concentrations, when
514 required: gentamicin (Gm) 30 µg/mL, carbenicillin (Carb) 200 µg/mL, or gentamicin (Gm) 15
515 µg/mL for *E. coli*. L- arabinose was added to media at a concentration of 0.2% (w/v), when
516 required, to induce expression from the pBADGr Ara promoter. All bacterial strains and plasmids
517 used for this study are listed in **Table S1.**

518 **Phage genome sequencing and analysis**

519 Bacteriophage genomes were extracted and assembled as previously described (62).
520 Phage PO4 was amplified using *P. aeruginosa* PAO1 as the host strain. Phage genomic DNA was
521 extracted (Norgen Biotek Phage DNA Isolation Kit) and sequenced using the Illumina NextSeq
522 2000 platform (Microbial Genome Sequencing Center/SeqCenter, Pittsburgh, PA, USA).
523 Sequencing results were assembled using SPAdes (version 3.15.5) (98) and annotated using
524 Pharokka (version 1.7.3) (99). The annotated genome of PO4 is available at the following
525 GenBank accession number: PX259653.

526 **Molecular biology**

527 All primers used are listed in **Table S2.** Chromosomal mutants were generated as
528 previously described (100) with the exception of pEX18Gm constructs with $pilD^{3}$, $pilD^{6}$, $pilD^{9}$,
529 and $pilD^{12VAR}$. These *pilD* variants were synthesized (gBlock, IDT). The oligos were digested
530 with the indicated restriction enzymes and ligated into pEX18Gm digested using the same
531 restriction enzymes. Plasmid and chromosomal sequences were confirmed using Sanger
532 sequencing (McMaster Genomics Facility) or Oxford Nanopore whole-plasmid sequencing
533 (Plasmidsauras).

534 The PilA chimera construct was created by PCR amplification of PAO1 *pilA* using an
535 upstream primer that contained the leader sequence of *hxcT* and first 15 bases of mature PAO1
536 *pilA* and downstream primer corresponding to the end of PAO1 *pilA* (Table S1). Amplified
537 genomic DNA was digested with appropriate restriction enzymes and ligated to pBADGr
538 digested with the same enzymes. The plasmid was introduced into PAO1 *pilA::Tn5* by
539 electroporation as described previously (100) and transformants selected on plates containing
540 Gm as above.

541 **Selection of phage-resistant mutants**

542 *P. aeruginosa* PAO1 was inoculated from overnight subculture into 5 mL LB, and
543 incubated at 37°C with shaking (200 rpm) to an optical density at 600 nm (OD_{600}) of 0.6. When
544 target OD_{600} was reached, 100 µL of the liquid bacterial culture was combined with 12 mL of
545 0.6% LB agar and 10 µL of PO4 at concentration of 10^8 PFU in culture tubes and poured into
546 petri dishes. Plates were incubated at 21°C for an additional 24 h or until the appearance of

547 bacteriophage resistant colonies. Colonies were selected and grown on 1.5% LB agar, incubated
548 at 37°C. To confirm bacteriophage resistance, phage streaking assays were completed using the
549 phage resistant colonies. On 1.5% LB agar plates, 5 µL of PO4 at concentration of 10^8 PFU was
550 applied onto the surface in four evenly spread out spots. An inoculation loop was dipped into
551 liquid culture of resistant colonies and dragged across the plate, crossing each phage sample.
552 Plates were incubated overnight at 37°C and checked the following day for growth.

553 **Twitching motility assays**

554 Twitching motility assays were completed as previously described (39). In brief,
555 bacterial strains were stab-inoculated through cell-culture treated single well plates containing
556 1% LB agar. Standard twitching assay plates incubated at 37°C, overnight. LB was
557 supplemented with L-arabinose and Gm when required. To visualize the twitching zone, agar
558 was removed, and plates were stained with 1% crystal violet for 5 min before washing with
559 water to remove excess dye. Plates were imaged using a flatbed scanner.

560 Samples for extended-length twitching assays used to assess phenotypic reversion were
561 also stab inoculated through cell-culture treated single well plates containing 1% LB agar. These
562 plates were sealed with Parafilm and placed in a sealed zipper storage bag. After seven days of
563 room temperature incubation, in the dark, for any twitching zones present, approximately 1cm of
564 cell growth were collected using a sterile cotton swab and transferred to Gm supplemented media
565 to assess growth. Remaining intact twitching zones were visualized as above.

566 Twitching zones were measured using Image J, when indicated. Average areas were
567 graphed using GraphPad Prism (version 10.2.0). One-way ANOVA statistical analysis was
568 performed on the areas using GraphPad Prism ($p < 0.05$ is considered statistically significant).

569 **Whole genome sequencing and mutation analysis of PRMs**

570 Genomic DNA of *P. aeruginosa* PAO1 WT and phage resistant strains were extracted
571 using the Wizard Genomic DNA Purification Kit. PRMs and PAO1 WT were sequenced using
572 the Illumina NextSeq 2000 platform (Microbial Genome Sequencing Center/SeqCenter,
573 Pittsburgh, PA, USA). All samples had average sequencing coverage of at least 50 reads. breseq
574 (versions 0.35.4, 0.36.1, or 0.37.1) was used to identify mutations by comparing mutants
575 sequences to the reference WT PAO1 Burrows lab strain (53). To ensure variant calling results
576 were reliable, only those with more than 50 reads were included in the analysis unless specified
577 (101). When required, mutations were confirmed by PCR and DNA sequencing (Plasmidsaurus,
578 Oxford Nanopore).

579 **Multi-strain phage susceptibility assays**

580 Overnight cultures of bacteria were grown (1:1000) in liquid LB media and incubated at
581 37°C with shaking (200 rpm). Subcultures were standardized to OD_{600} of 0.5 in LB media. Phage
582 stocks were standardized to 10^8 PFU/mL and 10-fold serially diluted in phage buffer (68mM
583 NaCl, 10mM Tris-HCl pH7.5, 10 mM $CaCl_2$, and 10mM $MgSO_4$). Five µL each of culture and
584 phage were combined and spotted onto 0.6% LB agar plates and dried for 5 min before
585 incubation for 18-24 hours at 21°C. Phage susceptibility is indicated by absence of cell growth,
586 relative to the control.

587

588 **Single strain phage plaquing assays**

589 Overnight culture of bacteria were grown (1:100) in liquid LB media and incubated at
590 37°C with shaking (200 rpm). Subcultures were standardized to OD_{600} of 0.3 in LB media and
591 100 µL of diluted culture was mixed with 12 mL of 0.6% LB agar and poured into standard petri
592 dishes. LB agar was air dried in a biosafety cabinet. Phage stocks were standardized to 10^8
593 PFU/mL and serially diluted with phage buffer. Five µL of each dilution was spotted onto the
594 plates and air dried. Plates were incubated for 18 hours at 30°C. Phage susceptibility is indicated
595 by phage plaque clearance.

596 **Liquid phage susceptibility assay**

597 Strains of interest were combined with PO4 at MOI=1 in 100 µL LB. Samples were
598 grown shaking (orbital) at 37°C for 18 hours in the Biotek Epoch Plate readers. OD_{600}
599 measurements were taken every 30 minutes. OD_{600} measurements were graphed using Graphpad
600 Prism version 10.2.0. Phage susceptibility is indicated by lack of growth.

601 **Sheared surface protein analysis**

602 Sheared surface protein preparations were completed as previously described.[15] Each
603 strain/mutant was streaked on two 1.5% LB agar plates, containing L-arabinose and Gm when
604 required, in a grid and incubated overnight at 37°C. Cells were gently scraped using sterile
605 coverslips and resuspended into 3 mL of 1X phosphate buffered saline (PBS) to be vortexed for
606 15 s, twice. Samples were aliquoted into 1.5 mL Eppendorf tubes and centrifuged at 21,000 x *g*
607 for 30 min. Supernatant was transferred into new 1.5 mL Eppendorf tubes, 5M NaCl and 30%
608 (w/v) polyethylene glycol (8000) were each added to concentrations of 10% final volume.
609 Samples were incubated on ice for 60 min before centrifugation at 21,000 x *g* for 30 min to
610 precipitate proteins. Precipitated proteins were resuspended in 50 µL of sample loading buffer
611 (62.5mM TRIS-HCl pH 6.8, 2.5% SDS, 0.002% bromophenol blue, 5% β-mercaptoethanol, 10%
612 glycerol) and boiled for 10 min. Samples were cooled to room temperature before separation on
613 15% SDS-PAGE and visualized using Coomasie brilliant blue. Where pilin proteins could not be
614 detected on gels, their presence was confirmed using Western blot analysis, as described below.

615 **Whole cell protein sample analysis**

616 Bacterial strains were streaked on 1.5% LB agar plates and incubated overnight at 37°C.
617 Using an inoculating loop, bacteria were resuspended into 2 mL of 1X PBS and mixed. Samples
618 were diluted to an OD_{600} of 0.6 and 3mL transferred into 2 1.5 mL Eppendorf tubes before
619 centrifugation for 1 min at 21,000 x *g* . The supernatant was discarded and precipitated cells
620 were resuspended in 50 µL of 1X loading buffer. Samples were boiled for 10 min and cooled to
621 room temperature before separation with 15% SDS-PAGE, in 1X Tris-glycine running buffer
622 (diluted from 10X tris-glycine buffer containing 30.3 g tris, 144 g glycine, and 20 mL 10% SDS).
623 Following separation, proteins were transferred to a nitrocellulose membrane for 1 h at 225mA in
624 1X transfer buffer (20% methanol, 100mL of 10X tris-glycine buffer without SDS, in 1L of H_2O)
625 Membranes were blocked with 5% skim milk resuspended in 1X phosphate-buffer saline (PBS)
626 for minimum of 2 h, room temperature shaking. Primary antibodies were diluted in 1x PBS and
627 used in appropriate dilutions (α-PilA- 1:5000, α-PilB- 1:2000,), and incubated with the blot at
628 room temperature overnight. Membranes were washed 4x for 5 min with PBS followed by
629 incubation with 1:3000 dilution (1xPBS) of goat α-rabbit alkaline phosphatase-conjugated

630 secondary antibodies for 1 h at room temperate with shaking at 60 rpm. Membranes were washed
631 4 x for 5 min with 1x PBS before developing using 5-bromo-4-chloro-3-indoyl phosphate
632 (BCIP) and nitro blue tetrazolium chloride (NBT) resuspended in alkaline phosphatase buffer
633 (1mM Tris, 100mM NaCl, 5mM $MgCl_2$, pH 9.5), shaking in the dark for 10 minutes. Western
634 blots were imaged using a flatbed scanner.

635 **Time-course intracellular pilin processing analysis**

636 Overnight liquid bacterial cultures were grown in LB supplemented with 0.2% L-
637 arabinose and 30 mg/mL Gm and diluted to OD_{600} of 0.6 for timepoint 0 h and prepared as
638 described above. At each timepoint, cultures were diluted to OD_{600} of 0.6, if required, and
639 prepared as described above. Samples were separated using 16% Tris-Tricine gels in 1x running
640 buffer (diluted from 10X running buffer containing 24.2g Tris base, 17.9g tricine, 1g SDS)
641 instead of 15% SDS-PAGE gels (102). Following separation, proteins were transferred to a
642 nitrocellulose membrane for 1 h at 225 mA in 1X transfer buffer (20% methanol, 100mL of 10X
643 tris-glycine buffer without SDS, in 1L of H_2O) Membranes were blocked with 5% skim milk
644 resuspended in 1X phosphate-buffer saline (PBS) for minimum of 2 h, room temperature
645 shaking. Primary antibodies were diluted in 1x PBS and used in appropriate dilutions (α-PilA-
646 1:5000), and incubated with the blot at room temperature overnight. Membranes were washed 4x
647 for 5 min each with PBS followed by incubation with 1:3000 dilution (1xPBS) of goat α-rabbit
648 alkaline phosphatase-conjugated secondary antibodies for 1 h at room temperate with shaking at
649 60 rpm. Membranes were washed 4 x for 5 min each with 1x PBS before developing using 5-
650 bromo-4-chloro-3-indoyl phosphate (BCIP) and nitro blue tetrazolium chloride (NBT)
651 resuspended in alkaline phosphatase buffer (1mM Tris, 100mM NaCl, 5mM $MgCl_2$, pH 9.5),
652 shaking in the dark for 10 minutes. Western blots were imaged using a flatbed scanner.

653 **Protease secretion assay**

654 Skim milk media was created by combining 100 mL of 1.5% (w/v) skim milk powder in
655 deionized water and 100 mL LB supplemented with 1.5% tryptic soy agar (TSA), at room
656 temperature. (103) Media was poured onto rectangular single well plates and solidified. Bacteria
657 were inoculated in 5mL LB, and incubated with shaking (200 rpm) to an optical density at 600
658 nm (OD_{600}) of 0.5. Five µL of standardized bacterial culture was applied onto the skim milk
659 media and incubated at 21°C for 24 hours or until the appearance of clearance zones for control
660 samples. Plates were imaged using a flatbed scanner and quantified using ImageJ.

661 **Passaging and phage susceptibility of Resistant and Non-Twitching Strains (RANTS)**

662 Overnight cultures of RANTS were subcultured (1:000) in LB and incubated at 37°C
663 with shaking (200 rpm) for 5-8 h. Subcultures were diluted to assess phage susceptibility, as
664 described above. From the same overnight culture, 10 µL was diluted into 5 mL of LB and
665 incubated with shaking (200 rpm) overnight. The overnight culture was diluted to $OD_{600} = 0.6$
666 and phage spot assay was repeated, daily for 14 days.

667 **Insertion of the Gm resistance gene**

668 Prior to assessing the capacity of mutants to regain twitching motility following extended
669 incubations of up to 7 days, the strains were marked with a Gm resistance gene. Genomic
670 insertion using a mini-Tn7 vector was completed as previously described (104, 105). In short,
671 pUC18t-mini-Tn7T-Gm and pTNS1 were introduced by electroporation, and transformants were

recovered for 3.5 hours in LB. Cells were plated on 1.5% LB agar containing Gm overnight and successful insertion was confirmed by growth on supplemented media.

Data availability

The genome sequence of phage PO4 is available at NCBI GenBank accession number: PX259653.

Acknowledgements

We thank Ikram Qaderi for assistance in phage genome annotation, Dominique Tertigas for assistance in genome analysis, and Yaser Al Moayad for technical assistance with some experiments. This work was supported by a grant from the Canadian Institutes of Health Research to LLB (PJT-169053). LLB holds the Canada Research Chair in Microbe-Surface Interactions (CRC-2021-00103) and VNT holds a PGS-D award from the Natural Sciences and Engineering Research Council of Canada.

References

1. V. Pelicic, Type IV pili: e pluribus unum? *Mol. Microbiol.* **68**, 827–837 (2008).
2. R. Denise, S. S. Abby, E. P. C. Rocha, Diversification of the type IV filament superfamily into machines for adhesion, protein secretion, DNA uptake, and motility. *PLOS Biol.* **17**, e3000390 (2019).
3. L. L. Burrows, *Pseudomonas aeruginosa* Twitching Motility: Type IV Pili in Action. *Annu. Rev. Microbiol.* **66**, 493–520 (2012).
4. S. L. Gellatly, R. E. W. Hancock, *Pseudomonas aeruginosa* : new insights into pathogenesis and host defenses. *Pathog. Dis.* **67**, 159–173 (2013).
5. S. Burdman, O. Bahar, J. K. Parker, L. De La Fuente, Involvement of Type IV Pili in Pathogenicity of Plant Pathogenic Bacteria. *Genes* **2**, 706–735 (2011).
6. R. Kulkarni, *et al.*, Roles of Putative Type II Secretion and Type IV Pilus Systems in the Virulence of Uropathogenic *Escherichia coli*. *PLOS ONE* **4**, e4752 (2009).
7. D. E. Bradley, Basic Characterization of a *Pseudomonas aeruginosa* Pilus-Dependent Bacteriophage with a Long Noncontractile Tail. *J. Virol.* **12**, 1139–1148 (1973).
8. J. McCutcheon, D. Peters, J. Dennis, Identification and Characterization of Type IV Pili as the Cellular Receptor of Broad Host Range *Stenotrophomonas maltophilia* Bacteriophages DLP1 and DLP2. *Viruses* **10**, 338 (2018).
9. H. Harvey, *et al.*, *Pseudomonas aeruginosa* defends against phages through type IV pilus glycosylation. *Nat. Microbiol.* **3**, 47–52 (2018).
10. World Health Organization, *WHO Bacterial Priority Pathogens List 2024: Bacterial Pathogens of Public Health Importance, to Guide Research, Development, and Strategies to Prevent and Control Antimicrobial Resistance*, 1st ed (World Health Organization, 2024).
11. G. L. Winsor, *et al.*, Enhanced annotations and features for comparing thousands of *Pseudomonas genomes* in the *Pseudomonas* genome database. *Nucleic Acids Res.* **44**, D646-653 (2016).
12. C. L. Giltner, M. Habash, L. L. Burrows, *Pseudomonas aeruginosa* minor pilins are incorporated into type IV pili. *J. Mol. Biol.* **398**, 444–461 (2010).

714 13. M. S. Strom, D. Nunn, S. Lory, Multiple roles of the pilus biogenesis protein *pilD*:
715 involvement of *pilD* in excretion of enzymes from *Pseudomonas aeruginosa*. *J. Bacteriol.*
716 **173**, 1175–1180 (1991).
717 14. M. S. Strom, D. N. Nunn, S. Lory, A single bifunctional enzyme, PilD, catalyzes cleavage
718 and N-methylation of proteins belonging to the type IV pilin family. *Proc. Natl. Acad. Sci.*
719 *U. S. A.* **90**, 2404–2408 (1993).
720 15. J. C. Pepe, S. Lory, Amino acid substitutions in PilD, a bifunctional enzyme of
721 *Pseudomonas aeruginosa*. Effect on leader peptidase and N-methyltransferase activities *in*
722 *vitro* and *in vivo*. *J. Biol. Chem.* **273**, 19120–19129 (1998).
723 16. D. Nunn, S. Bergman, S. Lory, Products of three accessory genes, *pilB*, *pilC*, and *pilD*, are
724 required for biogenesis of *Pseudomonas aeruginosa* pili. *J. Bacteriol.* **172**, 2911–2919
725 (1990).
726 17. D. E. Bradley, Evidence for the retraction of *Pseudomonas aeruginosa* RNA phage pili.
727 *Biochem. Biophys. Res. Commun.* **47**, 142–149 (1972).
728 18. C. B. Whitchurch, J. S. Mattick, Characterization of a gene, *pilU*, required for twitching
729 motility but not phage sensitivity in *Pseudomonas aeruginosa*. *Mol. Microbiol.* **13**, 1079–
730 1091 (1994).
731 19. P. Chiang, M. Habash, L. L. Burrows, Disparate subcellular localization patterns of
732 *Pseudomonas aeruginosa* Type IV pilus ATPases involved in twitching motility. *J.*
733 *Bacteriol.* **187**, 829–839 (2005).
734 20. H. K. Takhar, K. Kemp, M. Kim, P. L. Howell, L. L. Burrows, The Platform Protein Is
735 Essential for Type IV Pilus Biogenesis. *J. Biol. Chem.* **288**, 9721–9728 (2013).
736 21. C. B. Whitchurch, M. Hobbs, S. P. Livingston, V. Krishnapillai, J. S. Mattick,
737 Characterisation of a *Pseudomonas aeruginosa* twitching motility gene and evidence for a
738 specialised protein export system widespread in eubacteria. *Gene* **101**, 33–44 (1991).
739 22. T. L. Leighton, R. N. C. Buensuceso, P. L. Howell, L. L. Burrows, Biogenesis of
740 *Pseudomonas aeruginosa* type IV pili and regulation of their function. *Environ. Microbiol.*
741 **17**, 4148–4163 (2015).
742 23. M. Ayers, *et al.*, PilM/N/O/P proteins form an inner membrane complex that affects the
743 stability of the *Pseudomonas aeruginosa* type IV pilus secretin. *J. Mol. Biol.* **394**, 128–142
744 (2009).
745 24. S. Tammam, *et al.*, PilMNOPQ from the *Pseudomonas aeruginosa* Type IV Pilus System
746 Form a Transenvelope Protein Interaction Network That Interacts with PilA. *J. Bacteriol.*
747 **195**, 2126–2135 (2013).
748 25. P. R. Martin, M. Hobbs, P. D. Free, Y. Jeske, J. S. Mattick, Characterization of *pilQ*, a new
749 gene required for the biogenesis of type 4 fimbriae in *Pseudomonas aeruginosa*. *Mol.*
750 *Microbiol.* **9**, 857–868 (1993).
751 26. J. Koo, *et al.*, Functional Mapping of PilF and PilQ in the *Pseudomonas aeruginosa* Type
752 IV Pilus System. *Biochemistry* **52**, 2914–2923 (2013).
753 27. L. Talà, A. Fineberg, P. Kukura, A. Persat, *Pseudomonas aeruginosa* orchestrates twitching
754 motility by sequential control of type IV pili movements. *Nat. Microbiol.* **4**, 774–780
755 (2019).
756 28. I. Zolfaghar, D. J. Evans, S. M. J. Fleiszig, Twitching Motility Contributes to the Role of
757 Pili in Corneal Infection Caused by *Pseudomonas aeruginosa*. *Infect. Immun.* **71**, 5389–
758 5393 (2003).

29. D. E. Bradley, Shortening of *Pseudomonas aeruginosa* Pili after RNA-Phage Adsorption. *J. Gen. Microbiol.* **72**, 303–319 (1972).
30. D. E. Bradley, The adsorption of *Pseudomonas aeruginosa* pilus-dependent bacteriophages to a host mutant with nonretractile pili. *Virology* **58**, 149–163 (1974).
31. M. Gutierrez-Rodarte, S. Kolappan, B. A. Burrell, L. Craig, The *Vibrio cholerae* minor pilin TcpB mediates uptake of the cholera toxin phage CTXϕ. *J. Biol. Chem.* **294**, 15698–15710 (2019).
32. H.-W. Bae, H.-J. Ki, S.-Y. Choi, Y.-H. Cho, Pilin regions that select for the small RNA phages in *Pseudomonas aeruginosa* type IV pilus. *J. Virol.* **99**, e01949-24 (2025).
33. S. T. Abedon, Bacteriophage Adsorption: Likelihood of Virion Encounter with Bacteria and Other Factors Affecting Rates. *Antibiotics* **12**, 723 (2023).
34. S. J. Labrie, J. E. Samson, S. Moineau, Bacteriophage resistance mechanisms. *Nat. Rev. Microbiol.* **8**, 317–327 (2010).
35. T. Reyes-Robles, *et al.*, *Vibrio cholerae* Outer Membrane Vesicles Inhibit Bacteriophage Infection. *J. Bacteriol.* **200** (2018).
36. T. Sawa, K. Moriyama, M. Kinoshita, Current status of bacteriophage therapy for severe bacterial infections. *J. Intensive Care* **12**, 44 (2024).
37. R. C. T. Wright, V.-P. Friman, M. C. M. Smith, M. A. Brockhurst, Resistance Evolution against Phage Combinations Depends on the Timing and Order of Exposure. *mBio* **10** (2019).
38. M. León, R. Bastías, Virulence reduction in bacteriophage resistant bacteria. *Front. Microbiol.* **06** (2015).
39. S. L. N. Kilmury, L. L. Burrows, Type IV pilins regulate their own expression via direct intramembrane interactions with the sensor kinase PilS. *Proc. Natl. Acad. Sci.* **113**, 6017–6022 (2016).
40. M. McCallum, S. Tammam, A. Khan, L. L. Burrows, P. L. Howell, The molecular mechanism of the type IVa pilus motors. *Nat. Commun.* **8**, 15091 (2017).
41. J. E. Walker, M. Saraste, M. J. Runswick, N. J. Gay, Distantly related sequences in the alpha- and beta-subunits of ATP synthase, myosin, kinases and other ATP-requiring enzymes and a common nucleotide binding fold. *EMBO J.* **1**, 945–951 (1982).
42. V. Jakovljevic, S. Leonardy, M. Hoppert, L. Søgaard-Andersen, PilB and PilT Are ATPases Acting Antagonistically in Type IV Pilus Function in *Myxococcus xanthus*. *J. Bacteriol.* **190**, 2411–2421 (2008).
43. K. C. Cady, J. Bondy-Denomy, G. E. Heussler, A. R. Davidson, G. A. O'Toole, The CRISPR/Cas adaptive immune system of *Pseudomonas aeruginosa* mediates resistance to naturally occurring and engineered phages. *J. Bacteriol.* **194**, 5728–5738 (2012).
44. K. M. Sztanko, *et al.*, Prophages express a type IV pilus component to provide anti-phage defence. [Preprint] (2024). Available at: https://www.biorxiv.org/content/10.1101/2024.03.29.587342v1 [Accessed 24 March 2025].
45. M. S. Strom, P. Bergman, S. Lory, Identification of active-site cysteines in the conserved domain of PilD, the bifunctional type IV pilin leader peptidase/N-methyltransferase of *Pseudomonas aeruginosa*. *J. Biol. Chem.* **268**, 15788–15794 (1993).
46. S. Lory, M. S. Strom, Structure-function relationship of type-IV prepilin peptidase of *Pseudomonas aeruginosa*--a review. *Gene* **192**, 117–121 (1997).

47. D. N. Nunn, S. Lory, Cleavage, methylation, and localization of the *Pseudomonas aeruginosa* export proteins XcpT, -U, -V, and -W. *J. Bacteriol.* **175**, 4375–4382 (1993).
48. G. Ball, É. Durand, A. Lazdunski, A. Filloux, A novel type II secretion system in *Pseudomonas aeruginosa*. *Mol. Microbiol.* **43**, 475–485 (2002).
49. P. S. Pennings, C. B. Ogbunugafor, R. Hershberg, Reversion is most likely under high mutation supply when compensatory mutations do not fully restore fitness costs. *G3 GenesGenomesGenetics* **12**, jkac190 (2022).
50. G. Levinson, G. A. Gutman, Slipped-strand mispairing: a major mechanism for DNA sequence evolution. *Mol. Biol. Evol.* **4**, 203–221 (1987).
51. S. Bruzek, G. Vestal, A. Lasher, A. Lima, S. Silbert, Bacterial Whole Genome Sequencing on the Illumina iSeq 100 for Clinical and Public Health Laboratories. *J. Mol. Diagn.* **22**, 1419–1429 (2020).
52. A. W. Pightling, N. Petronella, F. Pagotto, Choice of Reference Sequence and Assembler for Alignment of *Listeria monocytogenes* Short-Read Sequence Data Greatly Influences Rates of Error in SNP Analyses. *PLOS ONE* **9**, e104579 (2014).
53. D. E. Deatherage, J. E. Barrick, Identification of mutations in laboratory evolved microbes from next-generation sequencing data using breseq. *Methods Mol. Biol. Clifton NJ* **1151**, 165–188 (2014).
54. J. E. Barrick, *et al.*, Identifying structural variation in haploid microbial genomes from short-read resequencing data using breseq. *BMC Genomics* **15**, 1039 (2014).
55. Barrick Lab, Frequently Asked Questions (FAQ) — breseq 0.35.0 documentation.
56. J. Bondy-Denomy, *et al.*, Prophages mediate defense against phage infection through diverse mechanisms. *ISME J.* **10**, 2854–2866 (2016).
57. J. Bertozzi Silva, Z. Storms, D. Sauvageau, Host receptors for bacteriophage adsorption. *FEMS Microbiol. Lett.* **363**, fnw002 (2016).
58. F. Forti, *et al.*, Identification and impact on *Pseudomonas aeruginosa* virulence of mutations conferring resistance to a phage cocktail for phage therapy. *Microbiol. Spectr.* **11**, e01477-23 (2023).
59. R. A. Alm, A. J. Bodero, P. D. Free, J. S. Mattick, Identification of a novel gene, *pilZ*, essential for type 4 fimbrial biogenesis in *Pseudomonas aeruginosa*. *J. Bacteriol.* (1996). https://doi.org/10.1128/jb.178.1.46-53.1996.
60. N. A. Roberge, L. L. Burrows, Building permits—control of type IV pilus assembly by PilB and its cofactors. *J. Bacteriol.* **206**, e00359-24 (2024).
61. R. C. T. Wright, V.-P. Friman, M. C. M. Smith, M. A. Brockhurst, Cross-resistance is modular in bacteria-phage interactions. *PLoS Biol.* **16**, e2006057 (2018).
62. I. Qaderi, I. Chan, H. Harvey, L. L. Burrows, Structural conservation and functional role of TfpY-like proteins in type IV pilus assembly. *J. Bacteriol.* **0**, e00343-24 (2025).
63. P. A. DeLange, T. L. Collins, G. E. Pierce, J. B. Robinson, PilJ localizes to cell poles and is required for type IV pilus extension in. *Curr. Microbiol.* **55**, 389–395 (2007).
64. K. E. Kortright, B. K. Chan, B. R. Evans, P. E. Turner, Arms race and fluctuating selection dynamics in *Pseudomonas aeruginosa* bacteria coevolving with phage OMKO1. *J. Evol. Biol.* **35**, 1475–1487 (2022).
65. H. R. Nordstrom, *et al.*, Genomic characterization of lytic bacteriophages targeting genetically diverse *Pseudomonas aeruginosa* clinical isolates. *iScience* **25**, 104372 (2022).

848 66. P. Chiang, *et al.*, Functional role of conserved residues in the characteristic secretion
849 NTPase motifs of the *Pseudomonas aeruginosa* type IV pilus motor proteins PilB, PilT
850 and PilU. *Microbiology* **154**, 114–126.
851 67. M. Shah, *et al.*, A phage-encoded anti-activator inhibits quorum sensing in *Pseudomonas*
852 *aeruginosa*. *Mol. Cell* **81**, 571-583.e6 (2021).
853 68. V. L. Taylor, *et al.*, "Prophages block cell surface receptors to ensure survival of their viral
854 progeny" (Microbiology, 2024).
855 69. P. Markwitz, *et al.*, Genome-driven elucidation of phage-host interplay and impact of phage
856 resistance evolution on bacterial fitness. *ISME J.* **16**, 533–542 (2022).
857 70. M. Castledine, *et al.*, Parallel evolution of *Pseudomonas aeruginosa* phage resistance and
858 virulence loss in response to phage treatment *in vivo* and *in vitro*. *eLife* **11**, e73679 (2022).
859 71. S. L. N. Kilmury, L. L. Burrows, The *Pseudomonas aeruginosa* PilSR Two-Component
860 System Regulates Both Twitching and Swimming Motilities. *mBio* **9**, e01310-18 (2018).
861 72. D. Nabergoj, P. Modic, A. Podgornik, Effect of bacterial growth rate on bacteriophage
862 population growth rate. *MicrobiologyOpen* **7**, e00558 (2018).
863 73. X. Qin, *et al.*, Quorum sensing influences phage infection efficiency via affecting cell
864 population and physiological state. *J. Basic Microbiol.* **57**, 162–170 (2017).
865 74. B. Alberts, *et al.*, "The Shape and Structure of Proteins" in *Molecular Biology of the Cell.*
866 *4th Edition*, (Garland Science, 2002).
867 75. Jessca M. Cabading, Christopher M. Dade, Katrina T. Forest, Catalytic activity of the
868 prepilin peptidase PilD is required for full *P. aeruginosa* virulence in a nematode infection
869 model. (2015). https://doi.org/10.1101/2025.07.10.664072.
870 76. S. Hesse, *et al.*, Phage Resistance in Multidrug-Resistant *Klebsiella pneumoniae* ST258
871 Evolves via Diverse Mutations That Culminate in Impaired Adsorption. *mBio* **11**,
872 10.1128/mbio.02530-19 (2020).
873 77. F. Kunisch, *et al.*, Targeting *Pseudomonas aeruginosa* biofilm with an evolutionary trained
874 bacteriophage cocktail exploiting phage resistance trade-offs. *Nat. Commun.* **15**, 8572
875 (2024).
876 78. R. Gopalan-Nair, *et al.*, Changes in DNA methylation contribute to rapid adaptation in
877 bacterial plant pathogen evolution. *PLOS Biol.* **22**, e3002792 (2024).
878 79. P. Ni, *et al.*, DNA 5-methylcytosine detection and methylation phasing using PacBio
879 circular consensus sequencing. *Nat. Commun.* **14**, 4054 (2023).
880 80. M. U. Ahsan, A. Gouru, J. Chan, W. Zhou, K. Wang, A signal processing and deep learning
881 framework for methylation detection using Oxford Nanopore sequencing. *Nat. Commun.*
882 **15**, 1448 (2024).
883 81. A. Górski, *et al.*, The fall and rise of phage therapy in modern medicine. *Expert Opin. Biol.*
884 *Ther.* **19**, 1115–1117 (2019).
885 82. S. Uyttebroek, *et al.*, Safety and efficacy of phage therapy in difficult-to-treat infections: a
886 systematic review. *Lancet Infect. Dis.* **22**, e208–e220 (2022).
887 83. J.-P. Pirnay, *et al.*, Personalized bacteriophage therapy outcomes for 100 consecutive cases:
888 a multicentre, multinational, retrospective observational study. *Nat. Microbiol.* **9**, 1434–
889 1453 (2024).
890 84. P. Markwitz, *et al.*, Emerging Phage Resistance in *Pseudomonas aeruginosa* PAO1 Is
891 Accompanied by an Enhanced Heterogeneity and Reduced Virulence. *Viruses* **13**, 1332
892 (2021).

85. S. L. N. Kilmury, K. J. Graham, R. P. Lamers, L. T. MacNeil, L. L. Burrows, Hyperpiliation, not loss of pilus retraction, reduces *Pseudomonas aeruginosa*. *Microbiol. Spectr.* **13**, e02558-24.
86. H. Sato, K. Okinaga, H. Saito, Role of Pili in the Pathogenesis of *Pseudomonas aeruginosa* Burn Infection. *Microbiol. Immunol.* **32**, 131–139 (1988).
87. L. Blasco, *et al.*, Case report: Analysis of phage therapy failure in a patient with a *Pseudomonas aeruginosa* prosthetic vascular graft infection. *Front. Med.* **10** (2023).
88. T. Rose, *et al.*, Experimental phage therapy of burn wound infection: difficult first steps. *Int. J. Burns Trauma* **4**, 66–73 (2014).
89. H. Duyvejonck, *et al.*, Development of a qPCR platform for quantification of the five bacteriophages within bacteriophage cocktail 2 (BFC2). *Sci. Rep.* **9**, 13893 (2019).
90. K. V., V. K. Neela, Twitching motility of <i>Stenotrophomonas maltophilia<i> under iron limitation: *In-silico*, phenotypic and proteomic approaches. *Virulence* **11**, 104–112 (2020).
91. T. Lam, *et al.*, Competence pili in *Streptococcus pneumoniae* are highly dynamic structures that retract to promote DNA uptake. https://doi.org/10.1111/mmi.14718.
92. E. B. Purcell, R. W. McKee, E. Bordeleau, V. Burrus, R. Tamayo, Regulation of Type IV Pili Contributes to Surface Behaviors of Historical and Epidemic Strains of *Clostridium difficile*. *J. Bacteriol.* (2015). https://doi.org/10.1128/jb.00816-15.
93. R. Meng, *et al.*, Structural basis of *Acinetobacter* type IV pili targeting by an RNA virus. *Nat. Commun.* **15**, 2746 (2024).
94. S. J. Ahern, M. Das, T. S. Bhowmick, R. Young, C. F. Gonzalez, Characterization of Novel Virulent Broad-Host-Range Phages of *Xylella fastidiosa* and *Xanthomonas*. *J. Bacteriol.* **196**, 459–471 (2014).
95. M. Sistrom, *et al.*, Genomic and Gene-Expression Comparisons among Phage-Resistant Type-IV Pilus Mutants of *Pseudomonas syringae pathovar phaseolicola*. *PLOS ONE* **10**, e0144514 (2015).
96. J. L. Villalpando-Aguilar, G. Matos-Pech, I. López-Rosas, H. G. Castelán-Sánchez, F. Alatorre-Cobos, Phage Therapy for Crops: Concepts, Experimental and Bioinformatics Approaches to Direct Its Application. *Int. J. Mol. Sci.* **24**, 325 (2022).
97. S. A. Ranveer, *et al.*, Positive and negative aspects of bacteriophages and their immense role in the food chain. *Npj Sci. Food* **8**, 1 (2024).
98. A. Prjibelski, D. Antipov, D. Meleshko, A. Lapidus, A. Korobeynikov, Using SPAdes De Novo Assembler. https://doi.org/10.1002/cpbi.102.
99. G. Bouras, *et al.*, Pharokka: a fast scalable bacteriophage annotation tool. *Bioinformatics* **39**, btac776 (2023).
100. D. C. K. Chan, L. L. Burrows, Pseudomonas aeruginosa FpvB Is a High-Affinity Transporter for Xenosiderophores Ferrichrome and Ferrioxamine B. *mBio* **14**, e03149-22 (2022).
101. A. Petrackova, *et al.*, Standardization of Sequencing Coverage Depth in NGS: Recommendation for Detection of Clonal and Subclonal Mutations in Cancer Diagnostics. *Front. Oncol.* **9** (2019).
102. H. Schägger, Tricine–SDS-PAGE. *Nat. Protoc.* **1**, 16–22 (2006).
103. É. Durand, *et al.*, Type II Protein Secretion in *Pseudomonas aeruginosa* the Pseudopilus Is a Multifibrillar and Adhesive Structure. *J. Bacteriol.* (2003). https://doi.org/10.1128/JB.185.9.2749-2758.2003.

938 104. K.-H. Choi, *et al.*, A Tn7-based broad-range bacterial cloning and expression system. *Nat.*
939 *Methods* **2**, 443–448 (2005).
940 105. K.-H. Choi, H. P. Schweizer, mini-Tn7 insertion in bacteria with single attTn7 sites:
941 example *Pseudomonas aeruginosa*. *Nat. Protoc.* **1**, 153–161 (2006).
942

Table 1. Mutations identified in Phage Resistant Mutants (PRMs)

Gene	Function	Protein size (kDa)	Location of mutation (Total AA length)	Effect on protein	Mutation	Effect (gene)
pilB	assembly ATPase	62.3	R258FS (566)	frameshift - truncation	Δ4bp frameshift; 765-768 (1701)	premature stop codon
pilB	assembly ATPase	62.3	T278P (566)	point mutation	A832C (1701)	point mutant
pilB	assembly ATPase	62.3	D388A (566)	point mutation	A1163C (1701)	point mutant
pilC	platform protein	40.9	N66FS (374)	truncation (70aa)	Δ11bp; 198- 208 (1125)	FS→ premature stop codon
pilC	platform protein	40.9	F470FS	frameshift - truncation	ΔT817 (1125)	FS→ premature stop codon
pilD	pre-pilin peptidase	31.9	L110FS (290)	truncation (137aa); non functional	ΔC326 (C) 5-->4	Premature stop codon
pilD	pre-pilin peptidase	31.9	F184-V187 (290)	in frame insertion	(GCGGTGTTCGGC)1 →2; 548-559; 12bp duplication	Longer amino acid, in-frame insertion
pilT	retraction ATPase	38	S191FS (348)	in frame deletion-shorteneing	Δ12; 563-571 (1037)	shortening
pilM	alignment subcomplex protein	38	ΔL175-A180 (354)	in frame deletion-shorteneing	ΔC523-C540 (1065)	in frame deletion
pilM	alignment subcomplex protein	38	V168FS (354)	frameshift - truncation	ΔG501 (1065)	frameshift, premature stop codon
pilM	alignment subcomplex protein	38	G224FS (354)	frameshift - truncation	ΔG671(1065)	frameshift, premature stop codon
pilM	alignment subcomplex protein	38	Y256*(354)	premature termination	C768G (1065)	premature stop codon

pilN	alignment subcomplex protein	22.2	N5FS (198)	frameshift	Δ11bp; 12-22; frameshift (597)	FS → elongation
pilO	alignment subcomplex protein	22.8	E108* (207)	truncation	G322T (624)	nonsense mutation
pilP	alignment subcomplex protein	19.1	I42FS (174)	frameshift - truncation	Δ5 bp (124-128) (525)	frameshift, premature stop codon
pilQ	secretin	77.4	Q428* (714)	truncation (427aa)	C1282T	Premature stop codon
pilQ	secretin	77.4	T605P (714)	point mutation	A605C (2145)	point mutant
pilR	TCS	49.7	S139P (445)	point mutation	T415C (1338)	point mutant
pilR	TCS	49.7	T275P (445)	point mutation	A823C (1338)	point mutant
pilR	TCS	49.7	ΔL301-V305 (445)	in frame deletion-shorteneing	Δ15 bp (900-014) (1338)	shortening
pilS	sensor of TCS that regulates pilA levels	59	G490FS (530)	frameshift	Δ50 bp; 1461-1510 (1593)	FS → elongation
pilZ	pilus assembly/twitching regulator	12.9	I39FS (118)	frameshift - elongation	+T114 (357)	FS → elongation
pilF	OM lipoprotein	28.5	Y116-R120 (257)	in frame insertion	15 bp duplication; (CAGAAGCGCTACGAG)1→2; 345-359	elongation
pilA	major pilin subunit	15.5	E11* (149)	truncation (10aa)	G31T	nonsense mutation
pilA	major pilin subunit	15.5	Y117-E120 (149)	in frame insertion	+ 12bp (349-360) (450)	insertion
pilW	minor pilin	30.1	E129*	truncation	G385T (624)	nonsense mutation

pilY1	minor pilin, adhesion	126.6	F470FS (1161)	frameshift - truncation	Δ10 bp; 1409-1410 (3486)	FS→ premature stop codon
pilS-pilY1					Δ7559 bp	

Table 2. Secondary RANT BreSeq analysis results

RANT	**Phenotype (EX/IN)[a]**	**Gene mutated[b]**	**Effect (gene)**	**Location of mutation (Total AA length)**	**Effect on protein**
RANT 1	X/X	N/A			
RANT 2	X/X	*pilR*	(+1018A)	Q40FS	longer transcript
RANT 3	X/ YES	*pilB*	ΔT646	F216FS	Frameshift-shortening
RANT 4	X/ YES	N/A			
RANT 5	X/X	*pilR*	T415C	PS139P	point mutation
RANT 6	YES/YES	N/A			
RANT 7	X/YES	N/A			
RANT 8	YES/YES	*pilR*	A823C	T275P	point mutation

[a] EX=extracellular pili, IN=intracellular pilins, X=none detected, YES=detected on gel/blot
[b] N/A=no change in genomic sequence compared to the wild-type reference